

Observation of triple J/ψ meson production in proton-proton collisions

Received: 9 November 2021

Accepted: 14 October 2022

Published online: 19 January 2023


 Check for updates

The CMS Collaboration* 

Protons consist of three valence quarks, two up-quarks and one down-quark, held together by gluons and a sea of quark-antiquark pairs. Collectively, quarks and gluons are referred to as partons. In a proton-proton collision, typically only one parton of each proton undergoes a hard scattering – referred to as single-parton scattering – leaving the remainder of each proton only slightly disturbed. Here, we report the study of double- and triple-parton scatterings through the simultaneous production of three J/ψ mesons, which consist of a charm quark-antiquark pair, in proton-proton collisions recorded with the CMS experiment at the Large Hadron Collider. We observed this process – reconstructed through the decays of J/ψ mesons into pairs of oppositely charged muons – with a statistical significance above five standard deviations. We measured the inclusive fiducial cross-section to be 272^{+141}_{-104} (stat) ± 17 (syst) fb, and compared it to theoretical expectations for triple- J/ψ meson production in single-, double- and triple-parton scattering scenarios. Assuming factorization of multiple hard-scattering probabilities in terms of single-parton scattering cross-sections, double- and triple-parton scattering are the dominant contributions for the measured process.

High-energy particle accelerators are unique tools to study the structure of matter at the shortest distances. The most powerful accelerator today is the CERN Large Hadron Collider (LHC) that has so far collided beams of protons with energies of up to 6.5 TeV, resulting in centre-of-mass energies of up to 13 TeV. Protons are used in energy-frontier colliders because they are relatively easy to accelerate and keep in a circular orbit to enable high collision rates. However, they are not fundamental particles and, in fact, have a complicated quantum mechanical structure. Protons consist of three quarks, two up-type and one down-type, and gluons, which hold together the three valence quarks, as well as of a ‘sea’ of virtual quark-antiquark pairs, which are fundamental elements of the quantum vacuum. All these components are referred to as ‘partons’. In the standard picture of proton-proton (pp) collisions, typically only a few partons undergo a hard scattering with one another, with the remainders of each proton only slightly disturbed in the process. As the collision energy increases, the densities of gluons and sea quarks probed inside each proton grow

rapidly. Thus, at high enough energies, more than one pair of partons can undergo a hard scattering in a single pp collision, leading to the simultaneous and independent production of two or more particles with transverse momentum (p_T) and/or mass (m) above a few gigaelectronvolts. Double-parton scatterings (DPS) were first observed at the CERN Intersecting Storage Rings some 35 years ago^{1,2} and have been a subject of intense theoretical and experimental investigations ever since³. Numerous DPS processes have been studied in measurements with many combinations of pairs of heavy and/or high- p_T produced particles³. Triple-parton scatterings (TPSs), where three hard parton interactions take place simultaneously, have been proposed for study only recently⁴ and have not been experimentally explored yet. Studies of n -parton scattering (NPS) processes are important to elucidate the complicated inner structure of the proton and its evolution with energy^{5,6}. Many of these features, for example, the parton density profile in the plane transverse to the colliding beams, as well as the various correlations (in position, momentum, flavour, colour, spin

*A list of authors and their affiliations appears at the end of the paper.  e-mail: cms-publication-committee-chair@cern.ch

and so on) between individual partons, are very difficult to calculate theoretically, and can only be mapped out through experimental studies of NPS in different systems and for different numbers n of simultaneous scatterings³.

Measurements of such processes not only allow for a deeper understanding of the proton structure but also are of relevance at the LHC to predict backgrounds in rare standard-model processes, and in searches for new physics, in final states where multiple heavy particles are produced^{7,8}. This Article presents the experimental study of the simultaneous production of three massive particles originating in NPS, and the observation of triple- J/ψ meson production. The study of TPS via triple- J/ψ production provides input for further theoretical and experimental progress in understanding the NPS dynamics.

In the simplest approach, ignoring any correlations between the individual partons, the probability to produce n high- p_T particles in a given pp collision must be proportional to the n th product of probabilities to independently produce each of them. Thus, the probability to produce two or three high- p_T particles in DPS and TPS scales with the square and cube, respectively, of the corresponding single-parton scattering (SPS) probabilities⁹. The occurrence of DPS and TPS processes is therefore more likely for final states with large SPS cross-sections, such as quarkonia states (for example, J/ψ and Υ mesons), than for rarer heavier particles, such as electroweak bosons¹⁰. In the DPS case, the cross-section to produce, for example, two charmonium mesons ψ_1 and ψ_2 can be written as the product of the SPS cross-sections for the production of each individual meson divided by an effective cross-section to warrant the proper units of the final result

$$\sigma_{\text{DPS}}^{\text{pp} \rightarrow \psi_1 \psi_2 + X} = \left(\frac{m}{2} \right) \frac{\sigma_{\text{SPS}}^{\text{pp} \rightarrow \psi_1 + X} \sigma_{\text{SPS}}^{\text{pp} \rightarrow \psi_2 + X}}{\sigma_{\text{eff,DPS}}} \quad (1)$$

Here, m is a combinatorial factor to avoid double counting, $m = 1$ (2) if $\psi_1 = \psi_2$ ($\psi_1 \neq \psi_2$), and $\sigma_{\text{eff,DPS}}$ is an effective cross-section that, in a purely geometric approach, can be determined from the pp transverse overlap⁹. A smaller value of $\sigma_{\text{eff,DPS}}$, which is proportional to the average (squared) transverse separation of the partons participating in the two hard scatterings, implies larger DPS yields.

For the proton form factors typically implemented in the Pythia^{8,11} and Herwig++¹² event generators commonly used in collider physics, values of $\sigma_{\text{eff,DPS}} \approx 20\text{--}30$ mb are expected. Such estimates are, however, about a factor of two larger than those experimentally derived via the ratio $\sigma_{\text{eff,DPS}} = (\sigma_{\text{SPS}}^{\text{pp} \rightarrow X_1} \sigma_{\text{SPS}}^{\text{pp} \rightarrow X_2}) / \sigma_{\text{DPS}}^{\text{pp} \rightarrow X_1 X_2}$ for processes involving pairs of high- p_T jets and/or electroweak bosons, which are found to lie in the range $\sigma_{\text{eff,DPS}} \approx 10\text{--}20$ mb (refs. 13–19). This discrepancy has been mostly explained as evidence of parton correlations in the collision not accounted for in the purely geometrical approaches²⁰. In addition, significantly lower $\sigma_{\text{eff,DPS}} \approx 3\text{--}10$ mb values have been extracted from measurements of quarkonium pair production ($J/\psi J/\psi$ (refs. 21–25), $J/\psi \Upsilon$ (ref. 26) and $\Upsilon \Upsilon$ (refs. 8,27)) that have been interpreted as due to the different dominant species (mostly gluons for quarkonia, and quarks for electroweak bosons) in the parton distribution functions (PDFs) probed in the different scatterings³, but can be also attributed in some cases to poorly controlled subtractions of SPS contributions¹⁰.

The study of TPS via triple- J/ψ production can help solve all the issues mentioned above. The equivalent of equation (1) for the production of three charmonium mesons in a TPS process reads

$$\sigma_{\text{TPS}}^{\text{pp} \rightarrow \psi_1 \psi_2 \psi_3 + X} = \left(\frac{m}{3!} \right) \frac{\sigma_{\text{SPS}}^{\text{pp} \rightarrow \psi_1 + X} \sigma_{\text{SPS}}^{\text{pp} \rightarrow \psi_2 + X} \sigma_{\text{SPS}}^{\text{pp} \rightarrow \psi_3 + X}}{\sigma_{\text{eff,TPS}}^2}, \quad (2)$$

where $m = 1, 3$ or 6 (depending on whether all three, two or none of the ψ_i states are identical). In the absence of parton correlations, the effective cross-section $\sigma_{\text{eff,TPS}}$ is closely related to its DPS counterpart via

$\sigma_{\text{eff,TPS}} = \kappa \sigma_{\text{eff,DPS}}$, with κ of order unity. A value of $\kappa = 0.82 \pm 0.11$ has been derived in ref. 4 for a variety of proton transverse parton profiles. A theoretical study of the production of three prompt- J/ψ mesons²⁸, based on the non-relativistic quantum chromodynamics approach at leading-order (LO) accuracy as implemented in the HELAC-Onia code^{29,30}, has demonstrated that the pure SPS contributions are negligible compared with those from DPS and TPS. Namely, the top left diagram of Fig. 1 is irrelevant compared with the two other diagrams in the left column of the figure. The experimental measurement of $\text{pp} \rightarrow J/\psi J/\psi J/\psi X$ is thus a golden channel for the study of TPS and, in addition, provides an alternative extraction of $\sigma_{\text{eff,DPS}}$, thereby shedding light on the underlying dynamics of hard NPS. The production of J/ψ states can also proceed non-promptly through the decay of a beauty-quark (b) hadron. Notwithstanding a small branching fraction, $\mathcal{B}_{b \rightarrow J/\psi X} \approx 1\%$ (ref. 31), the cross-section to produce $b\bar{b}$ pairs is large at the LHC, $\sigma(\text{pp} \rightarrow b\bar{b} X) \approx 0.5$ mb (ref. 4). The contributions of such processes to inclusive triple- J/ψ production are schematically shown in Fig. 1 (diagrams to the right of the vertical dashed line).

This Article reports the observation of the simultaneous production of three J/ψ mesons in pp collisions. The analysis is based on a data sample collected at $\sqrt{s} = 13$ TeV by the Compact Muon Solenoid (CMS) experiment, corresponding to an integrated luminosity of 133 fb^{-1} . The J/ψ mesons are reconstructed in their dimuon decay mode over a fiducial phase space in transverse momenta ($p_T^{\mu, J/\psi}$) and (pseudo) rapidities ($|\eta^{\mu}|$ and $|\eta^{J/\psi}|$) defined to maximize the signal purity and the detector acceptance and efficiency. The analysis of the 6μ final state offers a very clean experimental signature for inclusive triple- J/ψ production, comprising prompt and non-prompt components. Methods provides more details on the experimental set-up and event reconstruction (the J/ψ candidates passing the triple- J/ψ selection criteria are shown in Extended Data Table 1).

The signal yield is extracted with a three-dimensional unbinned extended maximum likelihood fit of the $m_{\mu^+ \mu^-}$ distributions of all J/ψ candidates in the event over the $2.9 \text{ GeV} < m_{\mu^+ \mu^-} < 3.3 \text{ GeV}$ range. The expected J/ψ mass peaks are modelled with a Gaussian function with mean fixed to their nominal value ($m^{J/\psi} = 3.097 \text{ GeV}$)³¹ and the root-mean-square (RMS) width fixed to the resolution derived from the Monte Carlo (MC) simulation ($\sigma_m \approx 30 \text{ MeV}$). Given the very low number of events passing the selection, the mass mean and RMS width of the J/ψ mesons cannot be left as free parameters in the fit. The dimuon background is described with an exponential function^{23,32–35}. The fit has eight free parameters for the yields given by the combination of each of the three J/ψ candidates as being either signal or background. The extracted signal yield (red shaded areas in the $m_{\mu^+ \mu^-}$ distributions of Fig. 2) corresponds to $N_{\text{sig}}^{3J/\psi} = 5.0^{+2.6}_{-1.9}$ triple- J/ψ events, with $1.0^{+1.4}_{-0.8}$ background events. The statistical significance of the signal is evaluated using various methods. From the likelihood ratio of two fits (background-only imposing $N_{\text{sig}}^{3J/\psi} = 0$, and the default signal-plus-background), with the standard asymptotic formula³⁶ assuming that the conditions to apply Wilks' theorem³⁷ are satisfied, a significance of 6.7 standard deviations (s.d.) is obtained. The significance derived assuming a Poisson counting experiment yields 5.8 s.d., and it is found to be above 5.5 s.d. by using MC pseudoexperiments.

To cross-check the size of the combinatorial background derived from the fit, two tests are carried out. First, the fit is repeated over the extended dimuon mass range $[2.5\text{--}3.3] \text{ GeV}$ for the two subleading J/ψ mesons (dotted curves in Fig. 2). This mass range corresponds to an asymmetric window of about $[-20\sigma_m, +7\sigma_m]$ around the J/ψ nominal mass that, as aforementioned, covers lower dimuon masses where the background, if any, should be larger. The obtained signal yield is fully consistent with the default result. A second test is performed whereby the opposite-sign (OS) requirement is removed to allow also for same-sign dimuon combinations ($\mu^+ \mu^+$) for the two subleading pairs. After applying the rest of the selection criteria of the default analysis, no triplet events containing same-sign muon pairs are observed.

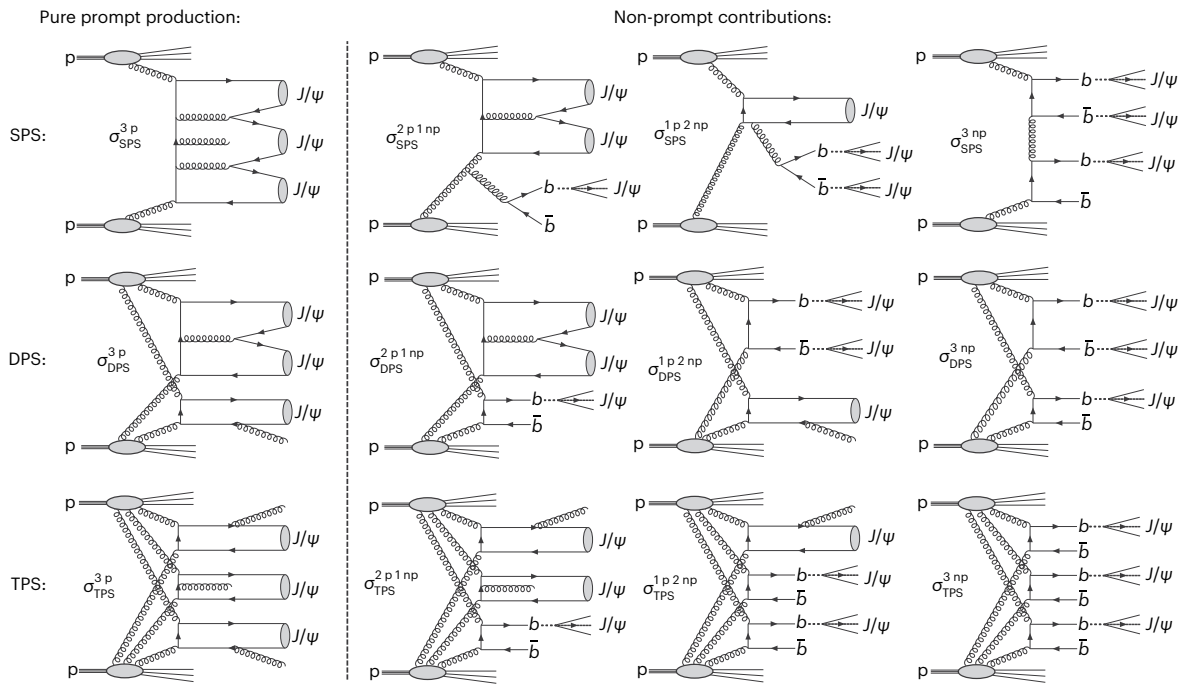


Fig. 1 | Leading-order diagrams for inclusive triple- J/ψ production in pp collisions. The SPS, DPS and TPS processes are depicted in the top, middle and bottom rows, respectively. The leftmost diagrams show triple prompt- J/ψ processes. The remaining diagrams show (left to right) final states with increasing contributions of non-prompt- J/ψ mesons from beauty hadron decays.

Curly lines indicate gluons, arrows indicate (anti)charm quarks and ovals indicate the proton parton densities. The symbols $\sigma_{NPS}^{i,j}$ identify the number (i and j) of prompt (p) and non-prompt (np) contributions to the cross-section of each diagram.

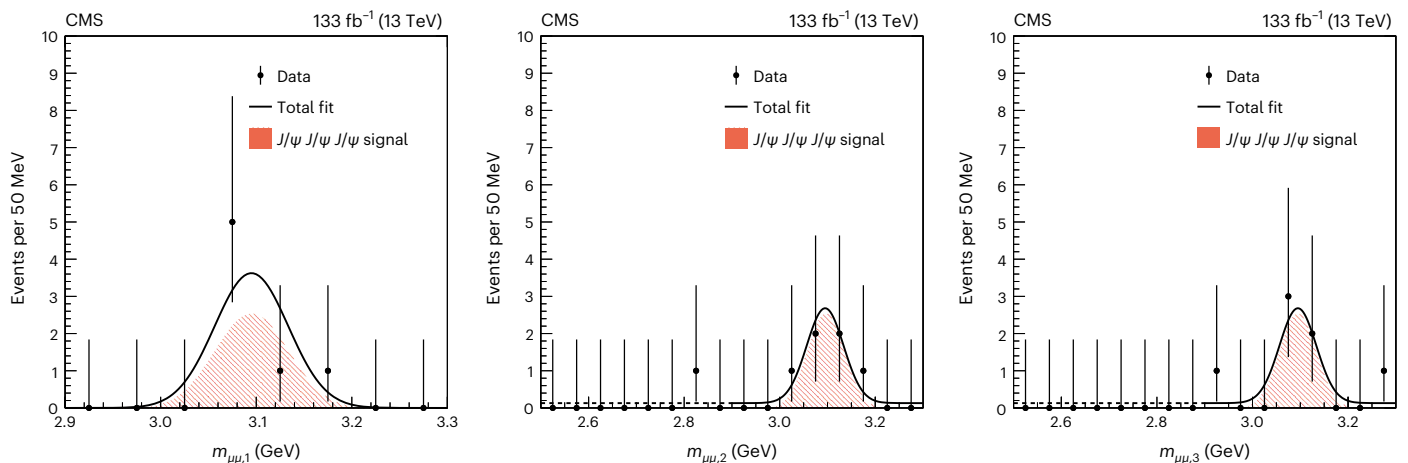


Fig. 2 | Invariant mass distributions for the three $\mu^+\mu^-$ pairs in the selected events. The three distributions are ordered, left to right, by decreasing pair p_T . The data are represented by the points with the vertical bars showing the (Poisson) statistical uncertainties. The solid (dotted) curve shows the overall fit to the data (in the extended mass range, discussed in the main text), and the red shaded area shows the fitted signal yield. The horizontal bin width is indicated on the vertical axis legend.

To estimate the average prompt and non-prompt contributions in the triple- J/ψ events, the proper decay length of each J/ψ is calculated as $L^{J/\psi} = (m^{J/\psi}/p_T^{J/\psi})L_{xy}^{J/\psi}$, where $L_{xy}^{J/\psi} = (\mathbf{r} \cdot \mathbf{p}_T^{J/\psi})/p_T^{J/\psi}$ is the transverse distance between the J/ψ decay vertex and the primary pp interaction vertex (PV) (\mathbf{r} is the vector from the PV to the J/ψ vertex). The experimental resolution on $L^{J/\psi}$ is about 20 μm . Prompt- J/ψ mesons are defined as those having $L^{J/\psi} < 60 \mu\text{m}$, a choice that reduces the non-prompt contribution by more than one order in magnitude³³. A signal-only subset of events is defined based on all J/ψ candidates

found in a narrower invariant mass region, within ± 3 s.d. around $m^{J/\psi}$, than that used in the default signal extraction. In this range, five triple- J/ψ events are found that can be classified as two events being consistent with the ‘2 non-prompt + 1 prompt J/ψ ’ hypothesis, and one event each in the ‘1 non-prompt + 2 prompt J/ψ ’, ‘3 non-prompt J/ψ ’ and ‘3 prompt J/ψ ’ categories. Such a classification is confirmed with a second method where prompt and non-prompt weights are extracted with the sPlot technique³⁸, exploiting an unbinned maximum likelihood fit of the $L^{J/\psi}$ distributions.

Table 1 | Fiducial phase space for the triple- J/ψ cross-section measurement

For all muons	$p_T > 3.5 \text{ GeV}$ for $ \eta < 1.2$
	$p_T > 2.5 \text{ GeV}$ for $1.2 < \eta < 2.4$
For all J/ψ mesons	$p_T > 6 \text{ GeV}$ and $ \eta < 2.4$
	$2.9 \text{ GeV} < m_{\mu^+\mu^-} < 3.3 \text{ GeV}$

The cross-section for inclusive triple- J/ψ production measured in the fiducial region defined in Table 1 is obtained via $\sigma(\text{pp} \rightarrow J/\psi/J/\psi/J/\psi X) = N_{\text{sig}}^{3J/\psi} / (\epsilon \mathcal{L}_{\text{int}} \mathcal{B}_{J/\psi \rightarrow \mu^+\mu^-}^3)$, where $N_{\text{sig}}^{3J/\psi}$ is the number of signal events, \mathcal{L}_{int} is the total integrated luminosity, $\mathcal{B}_{J/\psi \rightarrow \mu^+\mu^-}$ is the dimuon branching fraction and $\epsilon = \epsilon_{\text{trig}} \epsilon_{\text{id}} \epsilon_{\text{reco}}$ is the total efficiency composed of trigger, identification and reconstruction components, respectively. The J/ψ muon identification and reconstruction efficiencies are extracted with the tag-and-probe method using correction factors from the large inclusive $J/\psi \rightarrow \mu^+\mu^-$ data samples used in ref. ³⁹. As they depend on the p_T and η of the muons, they propagate into the final cross-section via two-dimensional maps, yielding $\epsilon_{\text{id}} \epsilon_{\text{reco}} = 0.78$. The trigger efficiency is found to be $\epsilon_{\text{trig}} = 0.84$ from a study of the MC samples.

The impact on the extracted cross-section of the choice of functions used to reproduce the shapes of the signal and background dimuon invariant masses is studied. For the signal, the Gaussian distribution is changed to a Crystal-Ball function⁴⁰ as well as to a Gaussian function with the RMS width left to vary in the fit. The background shape is changed from the default exponential to first- and zeroth-order polynomials. The relative differences in the cross-sections obtained from the alternative modelling for signal and background are 0.8% and 3.4%, respectively, and are assigned as corresponding systematic uncertainties. Uncertainties arising from the muon reconstruction and identification efficiencies are derived by allowing the tag-and-probe correction factors for each (p_T, η) bin to vary within their precision, and checking the effect on the extracted cross-section. The maximal variation observed is $\pm 1.0\%$. Varying the relative composition of double- and single- J/ψ meson production in the MC event sample used for the determination of the trigger efficiency leads to a 3.4% propagated uncertainty. Uncertainties of 1.6% and 3.0% are added from the integrated luminosity measurement^{41–43}, and from the simulated signal sample size, respectively. The uncertainty in the $\mathcal{B}_{J/\psi \rightarrow \mu^+\mu^-} = (5.961 \pm 0.033)\%$ value^{31–33} propagates into a 1.7% uncertainty in the cross-section. The total systematic uncertainty of the measured cross-section is 6.2%, obtained by adding all individual sources in quadrature (Extended Data Table 2). The measured cross-section for triple- J/ψ production, within the fiducial region defined in Table 1, is $\sigma(\text{pp} \rightarrow J/\psi/J/\psi/J/\psi X) = 272_{-104}^{+141}$ (stat) ± 17 (syst) fb

The total inclusive triple- J/ψ cross-section is expected to correspond to the sum of the contributions from the SPS, DPS and TPS processes schematically shown in Fig. 1, each of which contains various combinations of prompt (p) and non-prompt (np) J/ψ contributions

$$\begin{aligned} \sigma_{\text{tot}}^{3J/\psi} &= \sigma_{\text{SPS}}^{3J/\psi} + \sigma_{\text{DPS}}^{3J/\psi} + \sigma_{\text{TPS}}^{3J/\psi} \\ &= (\sigma_{\text{SPS}}^{3\text{p}} + \sigma_{\text{SPS}}^{2\text{p}1\text{np}} + \sigma_{\text{SPS}}^{1\text{p}2\text{np}} + \sigma_{\text{SPS}}^{3\text{np}}) \\ &\quad + (\sigma_{\text{DPS}}^{3\text{p}} + \sigma_{\text{DPS}}^{2\text{p}1\text{np}} + \sigma_{\text{DPS}}^{1\text{p}2\text{np}} + \sigma_{\text{DPS}}^{3\text{np}}) \\ &\quad + (\sigma_{\text{TPS}}^{3\text{p}} + \sigma_{\text{TPS}}^{2\text{p}1\text{np}} + \sigma_{\text{TPS}}^{1\text{p}2\text{np}} + \sigma_{\text{TPS}}^{3\text{np}}). \end{aligned} \tag{3}$$

Under the simplest assumption of factorization of multiple hard-scattering probabilities in terms of SPS cross-sections, the DPS and TPS contributions to triple- J/ψ production (last row of equation (3))

can be written through equations (1) and (2) as a combination of products of single- and double- J/ψ SPS cross-sections as

$$\begin{aligned} \sigma_{\text{DPS}}^{3J/\psi} &= \frac{m_1}{\sigma_{\text{eff,DPS}}} \\ &\times \left[\sigma_{\text{SPS}}^{2\text{p}} \sigma_{\text{SPS}}^{1\text{p}} + \sigma_{\text{SPS}}^{2\text{p}} \sigma_{\text{SPS}}^{1\text{np}} + \sigma_{\text{SPS}}^{1\text{p}} \sigma_{\text{SPS}}^{1\text{p}1\text{np}} \right. \\ &\quad \left. + \sigma_{\text{SPS}}^{1\text{p}1\text{np}} \sigma_{\text{SPS}}^{1\text{np}} + \sigma_{\text{SPS}}^{1\text{p}} \sigma_{\text{SPS}}^{2\text{np}} + \sigma_{\text{SPS}}^{2\text{np}} \sigma_{\text{SPS}}^{1\text{np}} \right], \end{aligned} \tag{4}$$

and

$$\begin{aligned} \sigma_{\text{TPS}}^{3J/\psi} &= \frac{m_3}{\sigma_{\text{eff,TPS}}^2} \left[(\sigma_{\text{SPS}}^{1\text{p}})^3 + (\sigma_{\text{SPS}}^{1\text{np}})^3 \right] \\ &\quad + \frac{m_2}{\sigma_{\text{eff,TPS}}^2} \left[(\sigma_{\text{SPS}}^{1\text{p}})^2 \sigma_{\text{SPS}}^{1\text{np}} + \sigma_{\text{SPS}}^{1\text{p}} (\sigma_{\text{SPS}}^{1\text{np}})^2 \right], \end{aligned} \tag{5}$$

with combinatorial prefactors $m_1 = 2/2 = 1$, $m_2 = 3/3! = 1/2$ and $m_3 = 1/3! = 1/6$. Therefore, from the eight individual SPS cross-sections for single-, double- and triple- J/ψ production, one can determine the total triple- J/ψ production cross-section via equations (3)–(5). The values of the relevant SPS cross-sections, each within the fiducial phase space defined in Table 1, are computed as described next and listed in Table 2.

The values of the SPS single, double and triple prompt- J/ψ cross-sections ($\sigma_{\text{SPS}}^{1\text{p}}$, $\sigma_{\text{SPS}}^{2\text{p}}$ and $\sigma_{\text{SPS}}^{3\text{p}}$) are obtained with HELAC-Onia at LO or at approximately next-to-leading-order (NLO*) accuracy^{44,45}. For the single prompt- J/ψ prediction ($\sigma_{\text{SPS}}^{1\text{p}}$), the theoretical calculations HO(data) in Table 2 are normalized with a parameterization⁴⁶ that reproduces the data measured in pp collisions at 7 TeV (refs. ^{34,47}), including all feed-down contributions from decays of heavier charmonium resonances. For the double and triple prompt- J/ψ processes, the HELAC-Onia calculations include only the $\psi(2S)$ feed-down because the χ_c decay contribution is only a few percent. All predictions for cross-sections of non-prompt- J/ψ meson production in beauty hadron decays ($\sigma_{\text{SPS}}^{1\text{np}}$, $\sigma_{\text{SPS}}^{2\text{np}}$ and $\sigma_{\text{SPS}}^{3\text{np}}$) have been obtained with MadGraph 5_aMC@NLO (v.2.6.6)⁴⁸ matrix elements, scaled by a factor of 1.15 to account for next-to-next-to-leading-order $b\bar{b}$ cross-section corrections⁴, combined with the Pythia 8.244 generator for parton shower and decays (including all feed-down quarkonium contributions)⁴⁵. Mixed prompt plus non-prompt cross-sections ($\sigma_{\text{SPS}}^{(p)Yn}$) are obtained from $J/\psi + b\bar{b}$ events generated with HELAC-Onia at LO in the colour-singlet model interfaced with Pythia 8.244 for the b quarks fragmentation into non-prompt- J/ψ mesons. The uncertainties include the (dominant) theoretical scale dependence and the (subdominant) PDF uncertainties of the CT14NLO set⁴⁹, except for the single prompt- J/ψ predictions that have a better precision because they are determined with an explicit fit of the non-relativistic quantum chromodynamics predictions to the LHC data⁴⁶ and have an associated 10% uncertainty of experimental origin. All these sources are treated as uncorrelated and the corresponding uncertainties are added in quadrature.

Using equations (4) and (5) with the SPS cross-sections listed in Table 2, and assuming that the effective DPS and TPS cross-sections are related by $\sigma_{\text{eff,TPS}} = (0.82 \pm 0.11) \sigma_{\text{eff,DPS}}$ (ref. ⁴) in a baseline approach that ignores parton correlations, one can extract the value of the effective DPS cross-section that yields the experimentally measured $\sigma_{\text{tot}}^{3J/\psi}$ value. Following such a procedure, the value $\sigma_{\text{eff,DPS}} = 2.7_{-1.0}^{+1.4} (\text{exp})_{-1.0}^{+1.5} (\text{theo}) \text{ mb}$ is derived, where the first uncertainty is due to the experimental $\sigma_{\text{tot}}^{3J/\psi}$ precision and the second is due to the propagation of all sources of theoretical uncertainties in the ingredients of equations (3)–(5).

The inclusive triple- J/ψ theoretical cross-sections and yields for each individual process contributing to the total production are listed in Table 3. The expected contributions from SPS, DPS and TPS processes to the total triple- J/ψ cross-section amount to about 6%, 74% and 20%, respectively. This confirms the conclusion of ref. ²⁸ that triple- J/ψ

Table 2 | Theoretical J/ψ , $J/\psi + J/\psi$, and $J/\psi + J/\psi + J/\psi$ cross-sections

SPS single- J/ψ production		SPS double- J/ψ production			SPS triple- J/ψ production			
HO(data)	MG5NLO + Py8	HO (NLO*)	HO(LO) + Py8	MG5NLO + Py8	HO(LO)	HO(LO) + Py8	HO(LO) + Py8	MG5NLO + Py8
σ_{SPS}^{1p}	$\sigma_{\text{SPS}}^{1np}$	σ_{SPS}^{2p}	$\sigma_{\text{SPS}}^{1p1np}$	$\sigma_{\text{SPS}}^{2np}$	σ_{SPS}^{3p}	$\sigma_{\text{SPS}}^{2p1np}$	$\sigma_{\text{SPS}}^{1p2np}$	$\sigma_{\text{SPS}}^{3np}$
$570 \pm 57 \text{ nb}$	$600^{+130}_{-220} \text{ nb}$	$40^{+80}_{-26} \text{ pb}$	$24^{+35}_{-16} \text{ fb}$	$430^{+95}_{-130} \text{ pb}$	$< 5 \text{ ab}$	$5.2^{+9.6}_{-3.3} \text{ fb}$	14^{+17}_{-8} ab	$12 \pm 4 \text{ fb}$

Predictions for single-, double- and triple- J/ψ production cross-sections in SPS processes, which pass the fiducial criteria listed in Table 1, derived from the HELAC-Onia (HO) and MadGraph 5_aMC@NLO (MG5NLO) matrix element calculators, complemented with the Pythia8 (Py8) parton shower, as described in the text.

Table 3 | Expected contributions to triple- J/ψ production

Process:	3 p	2 p+1 np	1 p+2 np	3 np	Total
$\sigma_{\text{SPS}}^{3//\psi} \text{ fb}$	<0.005	5.7	0.014	12	18
$N_{\text{SPS}}^{3//\psi}$	0.0	0.10	0.0	0.22	0.32
$\sigma_{\text{DPS}}^{3//\psi} \text{ fb}$	8.4	8.9	90	95	202
$N_{\text{DPS}}^{3//\psi}$	0.15	0.16	1.65	1.75	3.7
$\sigma_{\text{TPS}}^{3//\psi} \text{ fb}$	6.1	19.4	20.4	7.2	53
$N_{\text{TPS}}^{3//\psi}$	0.11	0.36	0.38	0.13	1.0
$\sigma_{\text{tot}}^{3//\psi} \text{ fb}$	15	34	110	114	272
$N_{\text{tot}}^{3//\psi}$	0.3	0.6	2.0	2.1	5.0

Central values of the predictions for triple- J/ψ production cross-sections (in fb) and yields from SPS, DPS (for $\sigma_{\text{eff,DPS}} = 2.7 \text{ mb}$) and TPS (for $\sigma_{\text{eff,TPS}} = 0.82 \times \sigma_{\text{eff,DPS}} = 2.2 \text{ mb}$) processes, and their total sum. The values are given in columns for combinations of n prompt and $(3-n)$ non-prompt- J/ψ mesons, the last column giving their corresponding sums. The DPS and TPS results are derived via equations (3)–(5) from the SPS cross-sections listed in Table 2 with $\sigma_{\text{eff,DPS}}$ chosen so that the sum of contributions yields a total cross-section equal to the experimental value of $\sigma_{\text{tot}}^{3//\psi}$. The expected yield, $N_{\text{SPS}}^{3//\psi}$, is given for an effective integrated luminosity of $\mathcal{L}_{\text{int}} = 87 \text{ fb}^{-1}$ for each contributing process. The last column lists the total cross-sections and yields for SPS, DPS, TPS and their sums.

production is a golden channel to study DPS and TPS, with minimal SPS contamination. The largest contributors to the triple- J/ψ cross-section are $\sigma_{\text{DPS}}^{3np}$ and $\sigma_{\text{DPS}}^{1p2np}$, accounting for about 33% each, $\sigma_{\text{TPS}}^{2p1np}$ and $\sigma_{\text{TPS}}^{1p2np}$ amounting to about 7% each, and $\sigma_{\text{SPS}}^{3np}$ representing about 4% of the total production. In terms of prompt and non-prompt contributions, the theoretical expectation for the production of three promptly produced J/ψ mesons is about 5% of the total yield, whereas the percentage expected for three non-prompt- J/ψ mesons is about 45%. The remaining half of the triple- J/ψ events are expected to be due to the combination of J/ψ mesons produced promptly and from beauty hadron decays. This result is consistent, within the large statistical uncertainties of the present dataset, with the combination of prompt and non-prompt- J/ψ mesons derived from the decay length of each dimuon candidate.

In Fig. 3, the $\sigma_{\text{eff,DPS}}$ value extracted here (red circle) is compared with the world data on effective DPS cross-sections derived from midrapidity measurements with quarkonium final states^{22,24,25,57–60} (blue symbols), as well as from processes with jets, photons and/or W bosons^{13–19,51–56} (black symbols). A few of the $\sigma_{\text{eff,DPS}}$ values plotted have been derived by more advanced phenomenological studies^{57–60} of the experimental quarkonium data. The effective cross-sections obtained from quarkonium measurements favour a smaller value of $\sigma_{\text{eff,DPS}} \approx 3\text{--}10 \text{ mb}$ compared with the $\sigma_{\text{eff,DPS}} \approx 10\text{--}20 \text{ mb}$ derived from harder or heavier final states. Such an apparent process-dependent $\sigma_{\text{eff,DPS}}$ value is suggestive of different parton transverse profiles, and/or correlations present, probed inside the proton at varying fractional momenta, given by $x = \sqrt{p_{T,V}^2 + m_V^2} e^{\eta}/\sqrt{s}$, for $V = J/\psi, \gamma, W, Z$. At midrapidity ($|\eta| < 2.5$), quarkonia are produced mostly in gluon-gluon scatterings carrying a fraction $x \approx 5 \times 10^{-4}$ of the proton momentum, whereas mostly quarks

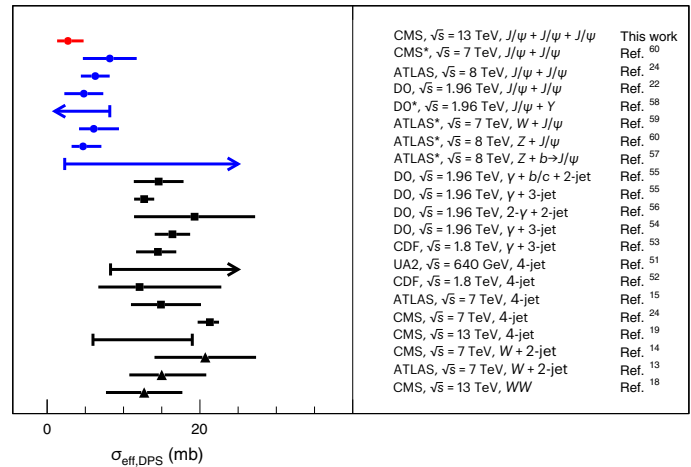


Fig. 3 | Comparison of $\sigma_{\text{eff,DPS}}$ parameters extracted in various processes.

The result obtained here (top red circle) is compared with those derived in midrapidity measurements of double-quarkonium and electroweak-boson-plus-quarkonium production^{22,24,25,57–60} (blue symbols), as well as in final states with jets^{19,51,52,62}, $\gamma + \text{jets}$ ^{53–56}, $W + \text{jets}$ ^{13,14} and same-sign W bosons¹⁸ (black symbols). The arrows indicate lower (or upper) limits at 95% (68%) confidence level. For the experimental results marked with a star, more recent theoretical reinterpretations based on more accurate calculations of the corresponding SPS cross-section are plotted. The original experimental results can be found in ref. 23 (CMS), ref. 26 (DO) and refs. 50,63 (ATLAS).

with $x \approx 10^{-2}$ participate in the production of electroweak bosons. The fact that LHCb measurements of double-quarkonia and quarkonia-plus-charm^{25,61} at forward rapidities ($\eta \approx 2\text{--}4.5$), processes that originate in parton scatterings with asymmetric fractional momenta $x_1 \approx 10^{-4}$ and $x_2 \approx 10^{-2}$, lead to values of $\sigma_{\text{eff,DPS}} \approx 15 \text{ mb}$, larger than those measured at midrapidity for similar final states, seems to confirm the dependence of the effective DPS cross-section on the relevant parton species and x fractions probed.

Online content

Any methods, additional references, Nature Portfolio reporting summaries, source data, extended data, supplementary information, acknowledgements, peer review information; details of author contributions and competing interests; and statements of data and code availability are available at <https://doi.org/10.1038/s41567-022-01838-y>.

References

- Åkesson, T. et al. Double parton scattering in pp collisions at $\sqrt{s} = 63 \text{ GeV}$. *Z. Phys. C* **34**, 163–174 (1987).
- Sjöstrand, T. & van Zijl, M. A multiple interaction model for the event structure in hadron collisions. *Phys. Rev. D* **36**, 2019–2041 (1987).
- Bartalini, P. & Gaunt, J. R. (eds) *Multiple Parton Interactions at the LHC* Vol. 29 (World Scientific, 2019); <https://doi.org/10.1142/10646>

4. d'Enterria, D. & Snigirev, A. M. Triple parton scatterings in high-energy proton-proton collisions. *Phys. Rev. Lett.* **118**, 122001 (2017).
5. Diehl, M., Ostermeier, D. & Schafer, A. Elements of a theory for multiparton interactions in QCD. *J. High Energy Phys.* **2012**, 089 (2012); erratum **2016**, 1 (2016).
6. Blok, B., Dokshitzer, Y., Frankfurt, L. & Strikman, M. pQCD physics of multiparton interactions. *Eur. Phys. J. C* **72**, 1963 (2012).
7. CMS Collaboration Search for Higgs and Z boson decays to J/ψ or Υ pairs in the four-muon final state in proton-proton collisions at $\sqrt{s} = 13$ TeV. *Phys. Lett. B* **797**, 134811 (2019).
8. CMS Collaboration Measurement of the $\Upsilon(1S)$ pair production cross section and search for resonances decaying to $\Upsilon(1S) \mu^+ \mu^-$ in proton-proton collisions at $\sqrt{s} = 13$ TeV. *Phys. Lett. B* **808**, 135578 (2020).
9. d'Enterria, D. & Snigirev, A. M. Double, triple, and n -parton scatterings in high-energy proton and nuclear collisions. *Adv. Ser. Direct. High. Energy Phys.* **29**, 159–187 (2018).
10. Chapon, E. et al. Perspectives for quarkonium studies at the high-luminosity LHC. *Prog. Part. Nucl. Phys.* **121**, 103906 (2021).
11. Sjöstrand, T. et al. An introduction to PYTHIA 8.2. *Comput. Phys. Commun.* **191**, 159–177 (2015).
12. Seymour, M. H. & Siodmok, A. Constraining MPI models using σ_{eff} and recent Tevatron and LHC underlying event data. *J. High Energy Phys.* **10**, 113 (2013).
13. ATLAS Collaboration Measurement of hard double-parton interactions in $W(\rightarrow lv) + 2$ jet events at $\sqrt{s} = 7$ TeV with the ATLAS detector. *New J. Phys.* **15**, 033038 (2013).
14. CMS Collaboration Study of double parton scattering using $W + 2$ -jet events in proton-proton collisions at $\sqrt{s} = 7$ TeV. *J. High Energy Phys.* **03**, 032 (2014).
15. ATLAS Collaboration Study of hard double-parton scattering in four-jet events in pp collisions at $\sqrt{s} = 7$ TeV with the ATLAS experiment. *J. High Energy Phys.* **11**, 110 (2016).
16. CMS Collaboration Constraints on the double-parton scattering cross section from same-sign W boson pair production in proton-proton collisions at $\sqrt{s} = 8$ TeV. *J. High Energy Phys.* **02**, 032 (2018).
17. ATLAS Collaboration Study of the hard double-parton scattering contribution to inclusive four-lepton production in pp collisions at $\sqrt{s} = 8$ TeV with the ATLAS detector. *Phys. Lett. B* **790**, 595–614 (2019).
18. CMS Collaboration Evidence for WW production from double-parton interactions in proton-proton collisions at $\sqrt{s} = 13$ TeV. *Eur. Phys. J. C* **80**, 41 (2020).
19. CMS Collaboration Measurement of double-parton scattering in inclusive production of four jets with low transverse momentum in proton-proton collisions at $\sqrt{s} = 13$ TeV. *J. High Energy Phys.* **01**, 177 (2022).
20. Blok, B. & Strikman, M. Multiparton pp and pA collisions: from geometry to parton-parton correlations. *Adv. Ser. Direct. High. Energy Phys.* **29**, 63–99 (2018).
21. LHCb Collaboration Observation of J/ψ pair production in pp collisions at $\sqrt{s} = 7$ TeV. *Phys. Lett. B* **707**, 52–59 (2012).
22. Abazov, V. M. et al. Observation and studies of double J/ψ production at the Tevatron. *Phys. Rev. D* **90**, 111101 (2014).
23. CMS Collaboration Measurement of prompt J/ψ pair production in pp collisions at $\sqrt{s} = 7$ TeV. *J. High Energy Phys.* **09**, 094 (2014).
24. ATLAS Collaboration Measurement of the prompt J/ψ pair production cross-section in pp collisions at $\sqrt{s} = 8$ TeV with the ATLAS detector. *Eur. Phys. J. C* **77**, 76 (2017).
25. LHCb Collaboration Measurement of the J/ψ pair production cross-section in pp collisions at $\sqrt{s} = 13$ TeV. *J. High Energy Phys.* **2017**, 047 (2017); erratum **2017**, 68 (2017).
26. Abazov, V. M. et al. Evidence for simultaneous production of J/ψ and Υ mesons. *Phys. Rev. Lett.* **116**, 082002 (2016).
27. CMS Collaboration Observation of $\Upsilon(1S)$ pair production in proton-proton collisions at $\sqrt{s} = 8$ TeV. *J. High Energy Phys.* **05**, 013 (2017).
28. Shao, H.-S. & Zhang, Y.-J. Triple prompt J/ψ hadroproduction as a hard probe of multiple-parton scatterings. *Phys. Rev. Lett.* **122**, 192002 (2019).
29. Shao, H.-S. HELAC-Onia: an automatic matrix element generator for heavy quarkonium physics. *Comput. Phys. Commun.* **184**, 2562–2570 (2013).
30. Shao, H.-S. HELAC-Onia 2.0: an upgraded matrix-element and event generator for heavy quarkonium physics. *Comput. Phys. Commun.* **198**, 238–259 (2016).
31. Zyla, P. A. et al. Review of particle physics. *Prog. Theor. Expt. Phys.* **2020**, 083C01 (2020).
32. CMS Collaboration Prompt and non-prompt J/ψ production in pp collisions at $\sqrt{s} = 7$ TeV. *Eur. Phys. J. C* **71**, 1575 (2011).
33. CMS Collaboration J/ψ and $\psi(2S)$ production in pp collisions at $\sqrt{s} = 7$ TeV. *J. High Energy Phys.* **02**, 011 (2012).
34. CMS Collaboration Measurement of J/ψ and $\psi(2S)$ prompt double-differential cross sections in pp collisions at $\sqrt{s} = 7$ TeV. *Phys. Rev. Lett.* **114**, 191802 (2015).
35. CMS Collaboration Measurement of prompt and nonprompt J/ψ production in pp and pPb collisions at $\sqrt{s_{\text{NN}}} = 5.02$ TeV. *Eur. Phys. J. C* **77**, 269 (2017).
36. Cowan, G., Cranmer, K., Gross, E. & Vitells, O. et al. Asymptotic formulae for likelihood-based tests of new. *Phys. Eur. Phys. J. C* **4**, 554 (2011).
37. Wilks, S. S. The large-sample distribution of the likelihood ratio for testing composite hypotheses. *Ann. Math. Stat.* **9**, 60–62 (1938).
38. Pivk, M. & LeDiberder, F. R. sPlot: a statistical tool to unfold data distributions. *Nucl. Instrum. Methods A* **555**, 356–369 (2005).
39. CMS Collaboration Performance of the CMS muon detector and muon reconstruction with proton-proton collisions at $\sqrt{s} = 13$ TeV. *J. Instrum.* **13**, 06015 (2018).
40. Oreglia, M. J. A Study of the Reactions $\psi' \rightarrow \gamma\gamma\psi$. PhD thesis, Stanford Univ. (1980); <http://www.slac.stanford.edu/cgi-wrap/getdoc/slac-r-236.pdf>
41. CMS Collaboration Precision luminosity measurement in proton-proton collisions at $\sqrt{s} = 13$ TeV in 2015 and 2016 at CMS. *Eur. Phys. J. C* **81**, 800 (2021).
42. CMS Collaboration CMS luminosity measurement for the 2017 data-taking period at $\sqrt{s} = 13$ TeV. CMS Physics Analysis Summary CMS-PAS-LUM-17-004 CERN Document Server <https://cds.cern.ch/record/2621960> (2017).
43. CMS Collaboration CMS luminosity measurement for the 2018 data-taking period at $\sqrt{s} = 13$ TeV. CMS Physics Analysis Summary CMS-PAS-LUM-18-002 CERN Document Server <https://cds.cern.ch/record/2676164> (2019).
44. Lansberg, J.-P. & Shao, H.-S. Production of $J/\psi + \eta_c$ versus $J/\psi + J/\psi$ at the LHC: importance of real α_s^2 corrections. *Phys. Rev. Lett.* **111**, 122001 (2013).
45. Lansberg, J.-P. & Shao, H.-S. J/ψ -pair production at large momenta: indications for double parton scatterings and large α_s^2 contributions. *Phys. Lett. B* **751**, 479–486 (2015).
46. Lansberg, J.-P. & Shao, H.-S. Towards an automated tool to evaluate the impact of the nuclear modification of the gluon density on quarkonium, D and B meson production in proton-nucleus collisions. *Eur. Phys. J. C* **77**, 1 (2017).
47. ATLAS Collaboration Measurement of the differential cross-sections of prompt and non-prompt production of J/ψ and $\psi(2S)$ in pp collisions at $\sqrt{s} = 7$ and 8 TeV with the ATLAS detector. *Eur. Phys. J. C* **76**, 283 (2016).

48. Alwall, J. et al. The automated computation of tree-level and next-to-leading order differential cross sections, and their matching to parton shower simulations. *J. High Energy Phys.* **07**, 079 (2014).
49. Dulat, S. et al. New parton distribution functions from a global analysis of quantum chromodynamics. *Phys. Rev. D* **93**, 033006 (2016).
50. ATLAS Collaboration Observation and measurements of the production of prompt and non-prompt J/ψ mesons in association with a Z boson in pp collisions at $\sqrt{s} = 8$ TeV with the ATLAS detector. *Eur. Phys. J. C* **75**, 229 (2015).
51. Alitti, J. et al. A study of multi-jet events at the CERN $\bar{p}p$ collider and a search for double parton scattering. *Phys. Lett. B* **268**, 145–154 (1991).
52. Abe, F. et al. Study of four jet events and evidence for double parton interactions in $\bar{p}p$ collisions at $\bar{p}p$ TeV. *Phys. Rev. D* **47**, 4857–4871 (1993).
53. Abe, F. et al. Double parton scattering in $\bar{p}p$ collisions at $\bar{p}p$ TeV. *Phys. Rev. D* **56**, 3811–3832 (1997).
54. Abazov, V. M. et al. Double parton interactions in $\gamma+3$ jet events in $\bar{p}p$ collisions $\bar{p}p$ TeV. *Phys. Rev. D* **81**, 052012 (2010).
55. Abazov, V. M. et al. Double parton interactions in $\gamma+3$ jet and $\gamma+b/c$ jet+2 jet events in $\bar{p}p$ collisions at $\bar{p}p$ TeV. *Phys. Rev. D* **89**, 072006 (2014).
56. Abazov, V. M. et al. Study of double parton interactions in diphoton + dijet events in $\bar{p}p$ collisions at $\bar{p}p$ TeV. *Phys. Rev. D* **93**, 052008 (2016).
57. Lansberg, J.-P. & Shao, H.-S. Phenomenological analysis of associated production of Z^0+b in the $b \rightarrow J/\psi X$ decay channel at the LHC. *Nucl. Phys. B* **916**, 132–142 (2017).
58. Shao, H.-S. & Zhang, Y.-J. Complete study of hadroproduction of a Y meson associated with a prompt J/ψ . *Phys. Rev. Lett.* **117**, 062001 (2016).
59. Lansberg, J.-P., Shao, H.-S. & Yamanaka, N. Indication for double parton scatterings in W +prompt J/ψ production at the LHC. *Phys. Lett. B* **781**, 485–491 (2018).
60. Lansberg, J.-P. New observables in inclusive production of quarkonia. *Phys. Rep.* **889**, 1–106 (2020).
61. LHCb Collaboration Observation of double charm production involving open charm in pp collisions at $\sqrt{s} = 7$ TeV. *J. High Energy Phys.* **2012**, 141 (2012); addendum **2014**, 108 (2014).
62. CMS Collaboration Event generator tunes obtained from underlying event and multiparton scattering measurements. *Eur. Phys. J. C* **76**, 155 (2016).
63. ATLAS Collaboration Measurement of the production cross section of prompt J/ψ mesons in association with a W^\pm boson in pp collisions at $\sqrt{s} = 7$ TeV with the ATLAS detector. *J. High Energy Phys.* **04**, 172 (2014).

Publisher's note Springer Nature remains neutral with regard to jurisdictional claims in published maps and institutional affiliations.

Open Access This article is licensed under a Creative Commons Attribution 4.0 International License, which permits use, sharing, adaptation, distribution and reproduction in any medium or format, as long as you give appropriate credit to the original author(s) and the source, provide a link to the Creative Commons license, and indicate if changes were made. The images or other third party material in this article are included in the article's Creative Commons license, unless indicated otherwise in a credit line to the material. If material is not included in the article's Creative Commons license and your intended use is not permitted by statutory regulation or exceeds the permitted use, you will need to obtain permission directly from the copyright holder. To view a copy of this license, visit <http://creativecommons.org/licenses/by/4.0/>.

© CERN 2023, for the benefit of the CMS Collaboration 2023

The CMS Collaboration

A. Tumasyan¹, W. Adam², J. W. Andrejkovic², T. Bergauer², S. Chatterjee², K. Damanakis², M. Dragicovic², A. Escalante Del Valle², R. Frühwirth^{2,216}, M. Jeitler^{2,216}, N. Krammer², L. Lechner², D. Liko², I. Mikulec², P. Paulitsch², F. M. Pitters², J. Schieck^{2,216}, R. Schöfbeck², D. Schwarz², S. Tempel², W. Waltenberger², C.-E. Wulz^{2,216}, V. Chekhovsky³, A. Litomin³, V. Makarenko³, M. R. Darwish^{4,217}, E. A. De Wolf⁴, T. Janssen⁴, T. Kello^{4,218}, A. Lelek⁴, H. Rejeb Sfar⁴, P. Van Mechelen⁴, S. Van Putte⁴, N. Van Remortel⁴, F. Blekman⁵, E. S. Bols⁵, J. D'Hondt⁵, M. Delcourt⁵, H. El Faham⁵, S. Lowette⁵, S. Moortgat⁵, A. Morton⁵, D. Müller⁵, A. R. Sahasransu⁵, S. Tavernier⁵, W. Van Doninck⁵, D. Beghin⁶, B. Bilin⁶, B. Clerbaux⁶, G. De Lentdecker⁶, L. Favart⁶, A. K. Kalsi⁶, K. Lee⁶, M. Mahdavihorrani⁶, I. Makarenko⁶, L. Moureaux⁶, L. Pêtré⁶, A. Popov⁶, N. Postiau⁶, E. Starling⁶, L. Thomas⁶, M. Vanden Bemden⁶, C. Vander Velde⁶, P. Vanlaer⁶, T. Cornelis⁷, D. Dobur⁷, J. Knolle⁷, L. Lambrecht⁷, G. Mestdach⁷, M. Niedziela⁷, C. Rendón⁷, C. Roskas⁷, A. Samalan⁷, K. Skovpen⁷, M. Tytgat⁷, B. Vermassen⁷, L. Wezenbeeck⁷, A. Benecke⁸, A. Bethani⁸, G. Bruno⁸, F. Bury⁸, C. Caputo⁸, P. David⁸, C. Delaere⁸, I. S. Donertas⁸, A. Giammanco⁸, K. Jaffel⁸, Sa. Jain⁸, V. Lemaître⁸, K. Mondal⁸, J. Prisciandaro⁸, A. Taliencio⁸, M. Teklishyn⁸, T. T. Tran⁸, P. Vischia⁸, S. Wertz⁸, G. A. Alves⁹, C. Hensel⁹, A. Moraes⁹, P. Rebello Teles⁹, W. L. Aldá Júnior¹⁰, M. Alves Gallo Pereira¹⁰, M. Barroso Ferreira Filho¹⁰, H. Brandao Malbousson¹⁰, W. Carvalho¹⁰, J. Chinellato^{10,219}, E. M. Da Costa¹⁰, G. G. Da Silveira^{10,220}, D. De Jesus Damiao¹⁰, V. Dos Santos Sousa¹⁰, S. Fonseca De Souza¹⁰, C. Mora Herrera¹⁰, K. Mota Amarilo¹⁰, L. Mundim¹⁰, H. Nogima¹⁰, A. Santoro¹⁰, S. M. Silva Do Amaral¹⁰, A. Sznajder¹⁰, M. Thiel¹⁰, F. Torres Da Silva De Araujo^{10,221}, A. Vilela Pereira¹⁰, C. A. Bernardes^{11,12,220}, L. Calligaris^{11,12}, T. R. Fernandez Perez Tomei^{11,12}, E. M. Gregores^{11,12}, D. S. Lemos^{11,12}, P. G. Mercadante^{11,12}, S. F. Novaes^{11,12}, Sandra S. Padula^{11,12}, A. Aleksandrov¹³, G. Antchev¹³, R. Hadjiiska¹³, P. Iaydjiev¹³, M. Misheva¹³, M. Rodozov¹³, M. Shopova¹³, G. Sultanov¹³, A. Dimitrov¹⁴, T. Ivanov¹⁴, L. Litov¹⁴, B. Pavlov¹⁴, P. Petkov¹⁴, A. Petrov¹⁴, T. Cheng¹⁵, T. Javaid^{15,222}, M. Mittal¹⁵, L. Yuan¹⁵, M. Ahmad¹⁶, G. Bauer¹⁶, C. Dozen^{16,223}, Z. Hu¹⁶, J. Martins^{16,224}, Y. Wang¹⁶, K. Yi^{16,225,226}, E. Chapon¹⁷, G. M. Chen^{17,222}, H. S. Chen^{17,222}, M. Chen¹⁷, F. Iemmi¹⁷, A. Kapoor¹⁷, D. Leggat¹⁷, H. Liao¹⁷, Z.-A. Liu^{17,222}, V. Milosevic¹⁷, F. Monti¹⁷, R. Sharma¹⁷, J. Tao¹⁷, J. Thomas-Wilsker¹⁷, J. Wang¹⁷, H. Zhang¹⁷, J. Zhao¹⁷, A. Agapitos¹⁸, Y. An¹⁸, Y. Ban¹⁸, C. Chen¹⁸, A. Levin¹⁸, Q. Li¹⁸, X. Lyu¹⁸, Y. Mao¹⁸, S. J. Qian¹⁸, D. Wang¹⁸, J. Xiao¹⁸, M. Lu¹⁹, Z. You¹⁹, X. Gao^{20,218}, H. Okawa²⁰, Y. Zhang²⁰, Z. Lin²¹, M. Xiao²¹, C. Avila²², A. Cabrera²², C. Florez²², J. Fraga²², J. Mejia Guisao²³, F. Ramirez²³, J. D. Ruiz Alvarez²³, C. A. Salazar González²³, D. Giljanovic²⁴, N. Godinovic²⁴, D. Lelas²⁴, I. Puljak²⁴, Z. Antunovic²⁵, M. Kovac²⁵, T. Sculac²⁵, V. Brigljevic²⁶, D. Ferencek²⁶, D. Majumder²⁶, M. Roguljic²⁶, A. Starodumov^{26,227}, T. Susa²⁶, A. Attikis²⁷, K. Christoforou²⁷, A. Ioannou²⁷, G. Kole²⁷, M. Kolosova²⁷, S. Konstantinou²⁷, J. Mousa²⁷, C. Nicolaou²⁷, F. Ptochos²⁷, P. A. Raziš²⁷, H. Rykaczewski²⁷, H. Saka²⁷, M. Finger^{28,228}, M. Finger Jr.^{28,228}, A. Kveton²⁸, E. Ayala²⁹, E. Carrera Jarrin³⁰, A. A. Abdelalim^{31,229,230}, S. Abu Zeid^{31,231},

M. A. Mahmoud³², Y. Mohammed³², S. Bhowmik³³, R. K. Dewanjee³³, K. Ehattat³³, M. Kadastik³³, S. Nandan³³, C. Nielsen³³, J. Pata³³, M. Raidal³³, L. Tani³³, C. Veelken³³, P. Eerola³⁴, H. Kirschenmann³⁴, K. Osterberg³⁴, M. Voutilainen³⁴, S. Bhattacharya³⁵, E. Brücken³⁵, F. Garcia³⁵, J. Havukainen³⁵, M. S. Kim³⁵, R. Kinnunen³⁵, T. Lampén³⁵, K. Lassila-Perini³⁵, S. Lehti³⁵, T. Lindén³⁵, M. Lotti³⁵, L. Martikainen³⁵, M. Myllymäki³⁵, J. Ott³⁵, H. Siikonen³⁵, E. Tuominen³⁵, J. Tuominiemi³⁵, P. Luukka³⁶, H. Petrow³⁶, T. Tuuva³⁶, C. Amendola³⁷, M. Besancon³⁷, F. Couderc³⁷, M. DeJardin³⁷, D. Denegri³⁷, J. L. Faure³⁷, F. Ferri³⁷, S. Ganjour³⁷, P. Gras³⁷, G. Hamel de Monchenault³⁷, P. Jarry³⁷, B. Lenzi³⁷, E. Locci³⁷, J. Malcles³⁷, J. Rander³⁷, A. Rosowsky³⁷, M. Ö. Sahin³⁷, A. Savoy-Navarro^{37,232}, M. Titov³⁷, G. B. Yu³⁷, S. Ahuja³⁸, F. Beaudette³⁸, M. Bonanomi³⁸, A. Buchot Perraguin³⁸, P. Busson³⁸, A. Cappati³⁸, C. Charlot³⁸, O. Davignon³⁸, B. Diab³⁸, G. Falmagne³⁸, S. Ghosh³⁸, R. Granier de Cassagnac³⁸, A. Hakimi³⁸, I. Kucher³⁸, J. Motta³⁸, M. Nguyen³⁸, C. Ochando³⁸, P. Paganini³⁸, J. Rembser³⁸, R. Salerno³⁸, U. Sarkar³⁸, J. B. Sauvan³⁸, Y. Sirois³⁸, A. Tarabini³⁸, A. Zabi³⁸, A. Zghiche³⁸, J.-L. Agram^{39,233}, J. Andrea³⁹, D. Apparú³⁹, D. Bloch³⁹, G. Bourgatte³⁹, J.-M. Brom³⁹, E. C. Chabert³⁹, C. Collard³⁹, D. Darej³⁹, J.-C. Fontaine^{39,233}, U. Goerlach³⁹, C. Grimault³⁹, A.-C. Le Bihan³⁹, E. Nibigira³⁹, P. Van Hove³⁹, E. Asilar⁴⁰, S. Beauceron⁴⁰, C. Berner⁴⁰, G. Boudoul⁴⁰, C. Camen⁴⁰, A. Carle⁴⁰, N. Chanon⁴⁰, D. Contardo⁴⁰, P. Depasse⁴⁰, H. El Mamouni⁴⁰, J. Fay⁴⁰, S. Gascon⁴⁰, M. Gouzevitch⁴⁰, B. Ille⁴⁰, I. B. Laktineh⁴⁰, H. Lattaud⁴⁰, A. Lesauvage⁴⁰, M. Lethuillier⁴⁰, L. Mirabito⁴⁰, S. Perries⁴⁰, K. Shchablo⁴⁰, V. Sordini⁴⁰, L. Torterotot⁴⁰, G. Touquet⁴⁰, M. Vander Donckt⁴⁰, S. Viret⁴⁰, I. Lomidze⁴¹, T. Toriashvili^{41,234}, Z. Tsamalaidze^{41,228}, V. Botta⁴², L. Feld⁴², K. Klein⁴², M. Lipinski⁴², D. Meuser⁴², A. Pauls⁴², N. Röwert⁴², J. Schulz⁴², M. Teroerde⁴², A. Dodonova⁴³, D. Eliseev⁴³, M. Erdmann⁴³, P. Fackeldey⁴³, B. Fischer⁴³, S. Ghosh⁴³, T. Hebbeker⁴³, K. Hoepfner⁴³, F. Ivone⁴³, L. Mastrolorenzo⁴³, M. Merschmeyer⁴³, A. Meyer⁴³, G. Mocellin⁴³, S. Mondal⁴³, S. Mukherjee⁴³, D. Noll⁴³, A. Novak⁴³, T. Pook⁴³, A. Pozdnyakov⁴³, Y. Rath⁴³, H. Reithler⁴³, J. Roemer⁴³, A. Schmidt⁴³, S. C. Schuler⁴³, A. Sharma⁴³, L. Vigilante⁴³, S. Wiedenbeck⁴³, S. Zaleski⁴³, C. Dziwok⁴⁴, G. Flügge⁴⁴, W. Haj Ahmad^{44,235}, O. Hlushchenko⁴⁴, T. Kress⁴⁴, A. Nowack⁴⁴, O. Pooth⁴⁴, D. Roy⁴⁴, A. Stahl^{44,236}, T. Ziemons⁴⁴, A. Zotz⁴⁴, H. Aarup Petersen⁴⁵, M. Aldaya Martin⁴⁵, P. Asmuss⁴⁵, S. Baxter⁴⁵, M. Bayatmakou⁴⁵, O. Behnke⁴⁵, A. Bermúdez Martínez⁴⁵, S. Bhattacharya⁴⁵, A. A. Bin Anuar⁴⁵, K. Borrás^{45,237}, D. Brunner⁴⁵, A. Campbell⁴⁵, A. Cardini⁴⁵, C. Cheng⁴⁵, F. Colombina⁴⁵, S. Consuegra Rodríguez⁴⁵, G. Correia Silva⁴⁵, V. Danilov⁴⁵, M. De Silva⁴⁵, L. Didukh⁴⁵, G. Eckerlin⁴⁵, D. Eckstein⁴⁵, L. I. Estevez Banos⁴⁵, O. Filatov⁴⁵, E. Gallo^{45,238}, A. Geiser⁴⁵, A. Giraldi⁴⁵, A. Grohsjean⁴⁵, M. Guthoff⁴⁵, A. Jafari^{45,239}, N. Z. Jomhari⁴⁵, H. Jung⁴⁵, A. Kasem^{45,237}, M. Kasemann⁴⁵, H. Kaveh⁴⁵, C. Kleinwort⁴⁵, R. Kogler⁴⁵, D. Krücker⁴⁵, W. Lange⁴⁵, J. Lidrych⁴⁵, K. Lipka⁴⁵, W. Lohmann^{45,240}, R. Mankel⁴⁵, J.-A. Melzer-Pellmann⁴⁵, M. Mendizabal Morentin⁴⁵, J. Metwally⁴⁵, A. B. Meyer⁴⁵, M. Meyer⁴⁵, J. Mnich⁴⁵, A. Mussgiller⁴⁵, Y. Otarid⁴⁵, D. Pérez Adán⁴⁵, D. Pitzl⁴⁵, A. Raspereza⁴⁵, B. Ribeiro Lopes⁴⁵, J. Rübenach⁴⁵, A. Saggio⁴⁵, A. Saibel⁴⁵, M. Savitskiy⁴⁵, M. Scham^{45,241}, V. Scheurer⁴⁵, S. Schnake⁴⁵, P. Schütze⁴⁵, C. Schwanenberger^{45,238}, M. Shchedrolosiev⁴⁵, R. E. Sosa Ricardo⁴⁵, D. Stafford⁴⁵, N. Tonon⁴⁵, M. Van De Klundert⁴⁵, R. Walsh⁴⁵, D. Walter⁴⁵, Q. Wang⁴⁵, Y. Wen⁴⁵, K. Wichmann⁴⁵, L. Wiens⁴⁵, C. Wissing⁴⁵, S. Wuchterl⁴⁵, R. Aggleton⁴⁶, S. Albrecht⁴⁶, S. Bein⁴⁶, L. Benato⁴⁶, P. Connor⁴⁶, K. De Leo⁴⁶, M. Eich⁴⁶, F. Feindt⁴⁶, A. Fröhlich⁴⁶, C. Garbers⁴⁶, E. Garutti⁴⁶, P. Gunnellini⁴⁶, M. Hajheidari⁴⁶, J. Haller⁴⁶, A. Hinzmann⁴⁶, G. Kasieczka⁴⁶, R. Klanner⁴⁶, T. Kramer⁴⁶, V. Kutzner⁴⁶, J. Lange⁴⁶, T. Lange⁴⁶, A. Lobanov⁴⁶, A. Malara⁴⁶, A. Nigamova⁴⁶, K. J. Pena Rodriguez⁴⁶, M. Rieger⁴⁶, O. Rieger⁴⁶, P. Schleper⁴⁶, M. Schröder⁴⁶, J. Schwandt⁴⁶, J. Sonneveld⁴⁶, H. Stadie⁴⁶, G. Steinbrück⁴⁶, A. Tews⁴⁶, I. Zoi⁴⁶, J. Bechtel⁴⁷, S. Brommer⁴⁷, M. Burkart⁴⁷, E. Butz⁴⁷, R. Caspart⁴⁷, T. Chwalek⁴⁷, W. De Boer^{47,316}, A. Dierlamm⁴⁷, A. Droll⁴⁷, K. El Morabit⁴⁷, N. Faltermann⁴⁷, M. Giffels⁴⁷, J. O. Gosewisch⁴⁷, A. Gottmann⁴⁷, F. Hartmann^{47,236}, C. Heidecker⁴⁷, U. Husemann⁴⁷, P. Keicher⁴⁷, R. Koppenhöfer⁴⁷, S. Maier⁴⁷, M. Metzler⁴⁷, S. Mitra⁴⁷, Th. Müller⁴⁷, M. Neukum⁴⁷, A. Nürnberg⁴⁷, G. Quast⁴⁷, K. Rabbertz⁴⁷, J. Rauser⁴⁷, D. Savoie⁴⁷, M. Schnepf⁴⁷, D. Seith⁴⁷, I. Shvetsov⁴⁷, H. J. Simonis⁴⁷, R. Ulrich⁴⁷, J. Van Der Linden⁴⁷, R. F. Von Cube⁴⁷, M. Wassmer⁴⁷, M. Weber⁴⁷, S. Wieland⁴⁷, R. Wolf⁴⁷, S. Wozniowski⁴⁷, S. Wunsch⁴⁷, G. Anagnostou⁴⁸, G. Daskalakis⁴⁸, T. Geralis⁴⁸, A. Kyriakis⁴⁸, D. Loukas⁴⁸, A. Stakia⁴⁸, M. Diamantopoulou⁴⁹, D. Karasavvas⁴⁹, P. Kontaxakis⁴⁹, C. K. Koraka⁴⁹, A. Manousakis-Katsikakis⁴⁹, A. Panagiotou⁴⁹, I. Papavergou⁴⁹, N. Saoulidou⁴⁹, K. Theofilatos⁴⁹, E. Tziaferi⁴⁹, K. Vellidis⁴⁹, E. Vourliotis⁴⁹, G. Bakas⁵⁰, K. Kousouris⁵⁰, I. Papakrivopoulos⁵⁰, G. Tsiolitis⁵⁰, A. Zacharopoulou⁵⁰, K. Adamidis⁵¹, I. Bestintzanos⁵¹, I. Evangelou⁵¹, C. Foudas⁵¹, P. Giannelis⁵¹, P. Katsoulis⁵¹, P. Kokkas⁵¹, N. Manthos⁵¹, I. Papadopoulos⁵¹, J. Strogos⁵¹, M. Csanad⁵², K. Farkas⁵², M. M. A. Gadallah^{52,242}, S. Lökös^{52,243}, P. Major⁵², K. Mandal⁵², A. Mehta⁵², G. Szzor⁵², A. J. Rádi⁵², O. Surányi⁵², G. I. Veres⁵², M. Bartók^{53,244}, G. Bencze⁵³, C. Hajdu⁵³, D. Horvath^{53,245}, F. Sikler⁵³, V. Veszpremi⁵³, S. Czellar⁵⁴, D. Fasanella⁵⁴, F. Fienga⁵⁴, J. Karancsi^{54,244}, J. Molnar⁵⁴, Z. Szillasi⁵⁴, D. Teysier⁵⁴, P. Raics⁵⁵, Z. L. Trocsanyi^{55,246}, B. Ujvari⁵⁵, T. Csorgo^{56,247}, F. Nemes^{56,247}, T. Novak⁵⁶, S. Choudhury⁵⁷, J. R. Komaragiri⁵⁷, D. Kumar⁵⁷, L. Panwar⁵⁷, P. C. Tiwari⁵⁷, S. Bahinipati^{58,248}, C. Kar⁵⁸, P. Mal⁵⁸, T. Mishra⁵⁸, V. K. Muraleedharan Nair Bindhu^{58,249}, A. Nayak^{58,249}, P. Saha⁵⁸, N. Sur⁵⁸, S. K. Swain⁵⁸, D. Vats^{58,249}, S. Bansal⁵⁹, S. B. Beri⁵⁹, V. Bhatnagar⁵⁹, G. Chaudhary⁵⁹, S. Chauhan⁵⁹, N. Dhingra^{59,250}, R. Gupta⁵⁹, A. Kaur⁵⁹, M. Kaur⁵⁹, P. Kumari⁵⁹, M. Meena⁵⁹, K. Sandeep⁵⁹, J. B. Singh⁵⁹, A. K. Virdi⁵⁹, A. Ahmed⁶⁰, A. Bhardwaj⁶⁰, B. C. Choudhary⁶⁰, M. Gola⁶⁰, S. Keshri⁶⁰, A. Kumar⁶⁰, M. Naimuddin⁶⁰, P. Priyanka⁶⁰, K. Ranjan⁶⁰, A. Shah⁶⁰, M. Bharti^{61,251}, R. Bhattacharya⁶¹, S. Bhattacharya⁶¹, D. Bhowmik⁶¹, S. Dutta⁶¹, S. Dutta⁶¹, B. Gomber^{61,252}, M. Maity^{61,253}, P. Palit⁶¹, P. K. Rout⁶¹, G. Saha⁶¹, B. Sahu⁶¹, S. Sarkar⁶¹, M. Sharan⁶¹, S. Thakur^{61,251}, P. K. Behera⁶², S. C. Behera⁶², P. Kalbhor⁶², A. Muhammad⁶², R. Pradhan⁶², P. R. Pujahari⁶², A. Sharma⁶², A. K. Sikdar⁶², D. Dutta⁶³, V. Jha⁶³, V. Kumar⁶³, D. K. Mishra⁶³, K. Naskar^{63,254}, P. K. Netrakanti⁶³, L. M. Pant⁶³, P. Shukla⁶³, T. Aziz⁶⁴, S. Dugad⁶⁴, M. Kumar⁶⁴, S. Banerjee⁶⁵, R. Chudasama⁶⁵, M. Guchait⁶⁵, S. Karmakar⁶⁵, S. Kumar⁶⁵, G. Majumder⁶⁵, K. Mazumdar⁶⁵, S. Mukherjee⁶⁵, K. Alpana⁶⁶, S. Dube⁶⁶, B. Kansal⁶⁶, A. Laha⁶⁶, S. Pandey⁶⁶, A. Rastogi⁶⁶, S. Sharma⁶⁶, H. Bakhshiansohi^{67,255}, E. Khazaie⁶⁷, M. Zeinali^{67,256}, S. Chenarani^{68,257}, S. M. Etesami⁶⁸, M. Khakzad⁶⁸, M. Mohammadi Najafabadi⁶⁸, M. Grunewald⁶⁹, M. Abbrescia^{70,71}, R. Aly^{70,71,258,259,260}, C. Aruta^{70,71}, A. Colaleo⁷⁰, D. Creanza^{70,72}, N. De Filippis^{70,72}, M. De Palma^{70,71}, A. Di Florio^{70,71}, A. Di Pilato^{70,71}, W. Elmetenawee^{70,71}, L. Fiore⁷⁰, A. Gelmi^{70,71}, M. Gul⁷⁰, G. Iaselli^{70,72}, M. Ince^{70,71}, S. Lezki^{70,71}, G. Maggi^{70,72}, M. Maggi⁷⁰, I. Margjeka^{70,71}, V. Mastrapasqua^{70,71}, S. My^{70,71}, S. Nuzzo^{70,71}, A. Pellecchia^{70,71}, A. Pompili^{70,71}, G. Pugliese^{70,72}, D. Ramos⁷⁰, A. Ranieri⁷⁰, G. Selvaggi^{70,71}, L. Silvestris⁷⁰, F. M. Simone^{70,71}, Å. Sözbilir⁷⁰, R. Venditti⁷⁰, P. Verwilligen⁷⁰, G. Abbiendi⁷³, C. Battilana^{73,74}, D. Bonacorsi^{73,74}, L. Borroni⁷³, L. Brigliadori⁷³, R. Campanini^{73,74}, P. Capiluppi^{73,74}, A. Castro^{73,74}, F. R. Cavallo⁷³, M. Cuffiani^{73,74}, G. M. Dallavalle⁷³, T. Diotallevi^{73,74}, F. Fabbri⁷³, A. Fanfani^{73,74}, P. Giacomelli⁷³, L. Giommi^{73,74}, C. Grandi⁷³, L. Guiducci^{73,74}, S. Lo Meo^{73,261}, L. Lunerti^{73,74}, S. Marcellini⁷³, G. Masetti⁷³, F. L. Navarra^{73,74}, A. Perrotta⁷³, F. Primavera^{73,74}, A. M. Rossi^{73,74}, T. Rovelli^{73,74}, G. P. Siroli^{73,74}, S. Albergo^{75,76,262}, S. Costa⁷⁵, A. Di Mattia⁷⁵, R. Potenza^{75,76}, A. Tricomi^{75,76}, C. Tuve^{75,76}, G. Barbagli⁷⁷, A. Cassese⁷⁷, R. Ceccarelli^{77,78}, V. Ciulli^{77,78}, C. Ciminini⁷⁷, R. D'Alessandro^{77,78}, E. Focardi^{77,78}, G. Latino^{77,78}, P. Lenzi^{77,78}, M. Lizzo^{77,78}, M. Meschini⁷⁷, S. Paoletti⁷⁷, R. Seidita^{77,78}, G. Sguazzoni⁷⁷, L. Viliani⁷⁷, L. Benussi⁷⁹, S. Bianco⁷⁹,

D. Piccolo⁷⁹, M. Bozzo^{80,81}, F. Ferro⁸⁰, R. Mulargia^{80,81}, E. Robutti⁸⁰, S. Tosi^{80,81}, A. Benaglia⁸², G. Boldrini⁸², F. Brivio^{82,83}, F. Cetorelli^{82,83}, F. De Guio^{82,83}, M. E. Dinardo^{82,83}, P. Dini⁸², S. Gennai⁸², A. Ghezzi^{82,83}, P. Govoni^{82,83}, L. Guzzi^{82,83}, M. T. Lucchini^{82,83}, M. Malberti⁸², S. Malvezzi⁸², A. Massironi⁸², D. Menasca⁸², L. Moroni⁸², M. Paganoni^{82,83}, D. Pedrini⁸², B. S. Pinolini⁸², S. Ragazzi^{82,83}, N. Redaelli⁸², T. Tabarelli de Fatis^{82,83}, D. Valsecchi^{82,83,236}, D. Zuolo^{82,83}, S. Buontempo⁸⁴, F. Carnevali^{84,85}, N. Cavallo^{84,86}, A. De Iorio^{84,85}, F. Fabozzi^{84,86}, A. O. M. Iorio^{84,85}, L. Lista^{84,85,263}, S. Meola^{84,87,236}, P. Paolucci^{84,236}, B. Rossi⁸⁴, C. Sciacca^{84,85}, P. Azzi⁸⁸, N. Bacchetta⁸⁸, D. Bisello^{88,89}, P. Bortignon⁸⁸, A. Bragagnolo^{88,89}, R. Carlin^{88,89}, P. Checchia⁸⁸, T. Dorigo⁸⁸, U. Dosselli⁸⁸, F. Gasparini^{88,89}, U. Gasparini^{88,89}, G. Grosso⁹⁰, S. Y. Hoh^{88,89}, L. Layer^{88,264}, E. Lusiani⁹⁰, M. Margoni^{88,89}, A. T. Meneguzzo^{88,89}, J. Pazzini^{88,89}, P. Ronchese^{88,89}, R. Rossin^{88,89}, F. Simonetto^{88,89}, G. Strong⁸⁸, M. Tosi^{88,89}, H. Yarar^{88,89}, M. Zanetti^{88,89}, P. Zotto^{88,89}, A. Zucchetta^{88,89}, G. Zumerle^{88,89}, C. Aimè^{91,92}, A. Braghieri⁹¹, S. Calzaferri^{91,92}, D. Fiorina^{91,92}, P. Montagna^{91,92}, S. P. Ratti^{91,92}, V. Re⁹¹, C. Riccardi^{91,92}, P. Salvini⁹¹, I. Vai⁹¹, P. Vitulo^{91,92}, P. Asenov^{93,265}, G. M. Bilei⁹³, D. Ciangottini^{93,94}, L. Fanò^{93,94}, M. Magherini⁹⁴, G. Mantovani^{93,94}, V. Mariani^{93,94}, M. Menichelli⁹³, F. Moscatelli⁹³, A. Piccinelli^{93,94}, M. Presilla^{93,94}, A. Rossi^{93,94}, A. Santocchia^{93,94}, D. Spiga⁹³, T. Tedeschi^{93,94}, P. Azzurri⁹⁵, G. Bagliesi⁹⁵, V. Bertacchi^{95,96}, L. Bianchini⁹⁵, T. Boccali⁹⁵, E. Bossini^{95,97}, R. Castaldi⁹⁵, M. A. Ciocci^{95,97}, V. D'Amante^{95,98}, R. Dell'Orso⁹⁵, M. R. Di Domenico^{95,98}, S. Donato⁹⁵, A. Giassi⁹⁵, F. Ligabue^{95,96}, E. Manca^{95,96}, G. Mandorli^{95,96}, D. Matos Figueiredo⁹⁵, A. Messineo^{95,97}, F. Palla⁹⁵, S. Parolia⁹⁵, G. Ramirez-Sanchez^{95,97}, A. Rizzi^{95,97}, G. Rolandi^{95,96}, S. Roy Chowdhury^{95,96}, A. Scribano⁹⁵, N. Shafiei^{95,97}, P. Spagnolo⁹⁵, R. Tenchini⁹⁵, G. Tonelli^{95,97}, N. Turini^{95,98}, A. Venturi⁹⁵, P. G. Verdini⁹⁵, P. Barria⁹⁹, M. Campana^{99,100}, F. Cavallari⁹⁹, D. Del Re^{99,100}, E. Di Marco⁹⁹, M. Diemoz⁹⁹, E. Longo^{99,100}, P. Meridiani⁹⁹, G. Organtini^{99,100}, F. Pandolfi⁹⁹, R. Paramatti^{99,100}, C. Quaranta^{99,100}, S. Rahatlou^{99,100}, C. Rovelli⁹⁹, F. Santanastasio^{99,100}, L. Soffi⁹⁹, R. Tramontano^{99,100}, N. Amapane^{101,102}, R. Arcidiacono^{101,103}, S. Argiro^{101,102}, M. Arneodo^{101,103}, N. Bartosik¹⁰¹, R. Bellan^{101,102}, A. Bellora^{101,102}, J. Berenguer Antequera^{101,102}, C. Biino¹⁰¹, N. Cartiglia¹⁰¹, M. Costa^{101,102}, R. Covarelli^{101,102}, N. Demaria¹⁰¹, B. Kiani^{101,102}, F. Legger¹⁰¹, C. Mariotti¹⁰¹, S. Maselli¹⁰¹, E. Migliore^{101,102}, E. Monteil^{101,102}, M. Monteno¹⁰¹, M. M. Obertino^{101,102}, G. Ortona¹⁰¹, L. Pacher^{101,102}, N. Pastrone¹⁰¹, M. Pelliccioni¹⁰¹, M. Ruspa^{101,103}, K. Shchelina¹⁰¹, F. Siviero^{101,102}, V. Sola¹⁰¹, A. Solano^{101,102}, D. Soldi^{101,102}, A. Staiano¹⁰¹, M. Tornago^{101,102}, D. Trocino¹⁰¹, A. Vagnerini^{101,102}, S. Belforte¹⁰⁴, V. Candelise^{104,105}, M. Casarsa¹⁰⁴, F. Cossutti¹⁰⁴, A. Da Rold^{104,105}, G. Della Ricca^{104,105}, G. Sorrentino^{104,105}, F. Vazzoler^{104,105}, S. Dogra¹⁰⁶, C. Huh¹⁰⁶, B. Kim¹⁰⁶, D. H. Kim¹⁰⁶, G. N. Kim¹⁰⁶, J. Kim¹⁰⁶, J. Lee¹⁰⁶, S. W. Lee¹⁰⁶, C. S. Moon¹⁰⁶, Y. D. Oh¹⁰⁶, S. I. Pak¹⁰⁶, S. Sekmen¹⁰⁶, Y. C. Yang¹⁰⁶, H. Kim¹⁰⁷, D. H. Moon¹⁰⁷, B. Francois¹⁰⁸, T. J. Kim¹⁰⁸, J. Park¹⁰⁸, S. Cho¹⁰⁹, S. Choi¹⁰⁹, B. Hong¹⁰⁹, K. Lee¹⁰⁹, K. S. Lee¹⁰⁹, J. Lim¹⁰⁹, J. Park¹⁰⁹, S. K. Park¹⁰⁹, J. Yoo¹⁰⁹, J. Goh¹¹⁰, A. Gurtu¹¹⁰, H. S. Kim¹¹¹, Y. Kim¹¹¹, J. Almond¹¹², J. H. Bhyun¹¹², J. Choi¹¹², S. Jeon¹¹², J. Kim¹¹², J. S. Kim¹¹², S. Ko¹¹², H. Kwon¹¹², H. Lee¹¹², S. Lee¹¹², B. H. Oh¹¹², M. Oh¹¹², S. B. Oh¹¹², H. Seo¹¹², U. K. Yang¹¹², I. Yoon¹¹², W. Jang¹¹³, D. Y. Kang¹¹³, Y. Kang¹¹³, S. Kim¹¹³, B. Ko¹¹³, J. S. H. Lee¹¹³, Y. Lee¹¹³, J. A. Merlin¹¹³, I. C. Park¹¹³, Y. Roh¹¹³, M. S. Ryu¹¹³, D. Song¹¹³, I. J. Watson¹¹³, S. Yang¹¹³, S. Ha¹¹⁴, H. D. Yoo¹¹⁴, M. Choi¹¹⁵, H. Lee¹¹⁵, Y. Lee¹¹⁵, I. Yu¹¹⁵, T. Beyrouthy¹¹⁶, Y. Maghrbi¹¹⁶, K. Dreimanis¹¹⁷, V. Veckalns^{117,266}, M. Ambrozias¹¹⁸, A. Carvalho Antunes De Oliveira¹¹⁸, A. Juodagalvis¹¹⁸, A. Rinkevicius¹¹⁸, G. Tamulaitis¹¹⁸, N. Bin Norjoharuddeen¹¹⁹, W. A. T. Wan Abdullah¹¹⁹, M. N. Yusli¹¹⁹, Z. Zolkapli¹¹⁹, J. F. Benitez¹²⁰, A. Castaneda Hernandez¹²⁰, M. León Coello¹²⁰, J. A. Murillo Quijada¹²⁰, A. Sehrawat¹²⁰, L. Valencia Palomo¹²⁰, G. Ayala¹²¹, H. Castilla-Valdez¹²¹, E. De La Cruz-Burelo¹²¹, I. Heredia-De La Cruz^{121,267}, R. Lopez-Fernandez¹²¹, C. A. Mondragon Herrera¹²¹, D. A. Perez Navarro¹²¹, A. Sánchez Hernández¹²¹, S. Carrillo Moreno¹²², C. Oropeza Barrera¹²², F. Vazquez Valencia¹²², I. Pedraza¹²³, H. A. Salazar Ibarquen¹²³, C. Uribe Estrada¹²³, J. Mijuskovic^{124,268}, N. Raicevic¹²⁴, D. Krofcheck¹²⁵, P. H. Butler¹²⁶, A. Ahmad¹²⁷, M. I. Asghar¹²⁷, A. Awais¹²⁷, M. I. M. Awan¹²⁷, H. R. Hoorani¹²⁷, W. A. Khan¹²⁷, M. A. Shah¹²⁷, M. Shoaib¹²⁷, M. Waqas¹²⁷, V. Avati¹²⁸, L. Grzanka¹²⁸, M. Malawski¹²⁸, H. Bialkowska¹²⁹, M. Bluj¹²⁹, B. Boimska¹²⁹, M. Górski¹²⁹, M. Kazana¹²⁹, M. Szleper¹²⁹, P. Zalewski¹²⁹, K. Bunkowski¹³⁰, K. Doroba¹³⁰, A. Kalinowski¹³⁰, M. Konecki¹³⁰, J. Krolikowski¹³⁰, M. Araujo¹³¹, P. Bargassa¹³¹, D. Bastos¹³¹, A. Boletti¹³¹, P. Faccioli¹³¹, M. Gallinaro¹³¹, J. Hollar¹³¹, N. Leonardo¹³¹, T. Niknejad¹³¹, M. Pisano¹³¹, J. Seixas¹³¹, O. Toldaiev¹³¹, J. Varela¹³¹, S. Afanasiev¹³², D. Budkouski¹³², I. Golutvin¹³², I. Gorbunov¹³², V. Karjavine¹³², V. Korenkov¹³², A. Lanev¹³², A. Malakhov¹³², V. Matveev^{132,269,270}, V. Palichik¹³², V. Perelygin¹³², M. Savina¹³², D. Seitova¹³², V. Shalaev¹³², S. Shmatov¹³², S. Shulha¹³², V. Smirnov¹³², O. Teryaev¹³², N. Voytishin¹³², B. S. Yuldashev^{132,271}, A. Zarubin¹³², I. Zhizhin¹³², G. Gavrillov¹³³, V. Golovtsov¹³³, Y. Ivanov¹³³, V. Kim^{133,272}, E. Kuznetsova^{133,273}, V. Murzin¹³³, V. Oreshkin¹³³, I. Smirnov¹³³, D. Sosnov¹³³, V. Sulimov¹³³, L. Uvarov¹³³, S. Volkov¹³³, A. Vorobyev¹³³, Yu. Andreev¹³⁴, A. Dermenev¹³⁴, S. Gninenko¹³⁴, N. Golubev¹³⁴, A. Karneyeu¹³⁴, D. Kirpichnikov¹³⁴, M. Kirsanov¹³⁴, N. Krasnikov¹³⁴, A. Pashenkov¹³⁴, G. Pivovarov¹³⁴, A. Toropin¹³⁴, V. Epshteyn¹³⁵, V. Gavrilov¹³⁵, N. Lychkovskaya¹³⁵, A. Nikitenko^{135,274}, V. Popov¹³⁵, A. Stepenov¹³⁵, M. Toms¹³⁵, E. Vlasov¹³⁵, A. Zhokin¹³⁵, T. Aushkevich¹³⁶, O. Bychkova¹³⁷, R. Chistov^{137,275}, M. Danilov^{137,275}, A. Oskina¹³⁷, P. Parygin¹³⁷, S. Polikarpov^{137,275}, V. Andreev¹³⁸, M. Azarkin¹³⁸, I. Dremin¹³⁸, M. Kirakosyan¹³⁸, A. Terkulov¹³⁸, A. Belyaev¹³⁹, E. Boos¹³⁹, M. Dubinin^{139,276}, L. Dudko¹³⁹, A. Ershov¹³⁹, A. Gribushin¹³⁹, V. Klyukhin¹³⁹, O. Kodolova¹³⁹, I. Lokhtin¹³⁹, S. Obraztsov¹³⁹, S. Petrushanko¹³⁹, V. Savrin¹³⁹, A. Snigirev¹³⁹, V. Blinov^{140,277}, T. Dimova^{140,277}, L. Kardapoltsev^{140,277}, A. Kozyrev^{140,277}, I. Ovtin^{140,277}, O. Radchenko^{140,277}, Y. Skovpen^{140,277}, I. Azhgirey¹⁴¹, I. Bayshev¹⁴¹, D. Elumakhov¹⁴¹, V. Kachanov¹⁴¹, D. Konstantinov¹⁴¹, P. Mandrik¹⁴¹, V. Petrov¹⁴¹, R. Ryutin¹⁴¹, S. Slabospitskii¹⁴¹, A. Sobol¹⁴¹, S. Troshin¹⁴¹, N. Tyurin¹⁴¹, A. Uzunian¹⁴¹, A. Volkov¹⁴¹, A. Babaev¹⁴², V. Okhotnikov¹⁴², V. Borshch¹⁴³, V. Ivanchenko¹⁴³, E. Tcherniaev¹⁴³, P. Adzic^{144,278}, M. Dordevic¹⁴⁴, P. Milenovic¹⁴⁴, J. Milosevic¹⁴⁴, M. Aguilar-Benitez¹⁴⁵, J. Alcaraz Maestre¹⁴⁵, A. Álvarez Fernández¹⁴⁵, I. Bachiller¹⁴⁵, M. Barrio Luna¹⁴⁵, Cristina F. Bedoya¹⁴⁵, C. A. Carrillo Montoya¹⁴⁵, M. Cepeda¹⁴⁵, M. Cerrada¹⁴⁵, N. Colino¹⁴⁵, B. De La Cruz¹⁴⁵, A. Delgado Peris¹⁴⁵, J. P. Fernández Ramos¹⁴⁵, J. Flix¹⁴⁵, M. C. Fouz¹⁴⁵, O. Gonzalez Lopez¹⁴⁵, S. Goy Lopez¹⁴⁵, J. M. Hernandez¹⁴⁵, M. I. Josa¹⁴⁵, J. León Holgado¹⁴⁵, D. Moran¹⁴⁵, Á. Navarro Tobar¹⁴⁵, C. Perez Dengra¹⁴⁵, A. Pérez-Calero Yzquierdo¹⁴⁵, J. Puerta Pelayo¹⁴⁵, I. Redondo¹⁴⁵, L. Romero¹⁴⁵, S. Sánchez Navas¹⁴⁵, L. Urda Gómez¹⁴⁵, C. Willmott¹⁴⁵, J. F. de Trocóniz¹⁴⁶, R. Reyes-Almanza¹⁴⁶, B. Alvarez Gonzalez¹⁴⁷, J. Cuevas¹⁴⁷, C. Erice¹⁴⁷, J. Fernandez Menendez¹⁴⁷, S. Folgueras¹⁴⁷, I. Gonzalez Caballero¹⁴⁷, J. R. González Fernández¹⁴⁷, E. Palencia Cortezon¹⁴⁷, C. Ramón Álvarez¹⁴⁷, V. Rodríguez Bouza¹⁴⁷, A. Soto Rodríguez¹⁴⁷, A. Trapote¹⁴⁷, N. Trevisani¹⁴⁷, C. Vico Villalba¹⁴⁷, J. A. Brochero Cifuentes¹⁴⁸, I. J. Cabrillo¹⁴⁸, A. Calderon¹⁴⁸, J. Duarte Campderros¹⁴⁸, M. Fernandez¹⁴⁸, C. Fernandez Madrazo¹⁴⁸, P. J. Fernández Manteca¹⁴⁸, A. García Alonso¹⁴⁸, G. Gomez¹⁴⁸, C. Martinez Rivero¹⁴⁸, P. Martinez Ruiz del Arbol¹⁴⁸, F. Matorras¹⁴⁸, P. Matorras Cuevas¹⁴⁸, J. Piedra Gomez¹⁴⁸, C. Prieels¹⁴⁸, A. Ruiz-Jimeno¹⁴⁸, L. Scodellaro¹⁴⁸, I. Vila¹⁴⁸, J. M. Vizan Garcia¹⁴⁸, M. K. Jayananda¹⁴⁹, B. Kailasapathy^{149,279}, D. U. J. Sonnadora¹⁴⁹, D. D. C. Wickramaratna¹⁴⁹, W. G. D. Dharmaratna¹⁵⁰, K. Liyanage¹⁵⁰, N. Perera¹⁵⁰, N. Wickramage¹⁵⁰, T. K. Aarrestad¹⁵¹, D. Abbaneo¹⁵¹, J. Alimena¹⁵¹, E. Auffray¹⁵¹, G. Auzinger¹⁵¹, J. Baechler¹⁵¹, P. Baillon^{151,317}, D. Barney¹⁵¹, J. Bendavid¹⁵¹, M. Bianco¹⁵¹, A. Bocchi¹⁵¹, C. Caillol¹⁵¹, T. Camporesi¹⁵¹, M. Capeans Garrido¹⁵¹,

A. Reinsvold Hall¹⁸³, L. Ristori¹⁸³, E. Sexton-Kennedy¹⁸³, N. Smith¹⁸³, A. Soha¹⁸³, L. Spiegel¹⁸³, S. Stoynev¹⁸³, J. Strait¹⁸³, L. Taylor¹⁸³, S. Tkaczyk¹⁸³, N. V. Tran¹⁸³, L. Uplegger¹⁸³, E. W. Vaandering¹⁸³, H. A. Weber¹⁸³, D. Acosta¹⁸⁴, P. Avery¹⁸⁴, D. Bourilkov¹⁸⁴, L. Cadamuro¹⁸⁴, V. Cherepanov¹⁸⁴, F. Errico¹⁸⁴, R. D. Field¹⁸⁴, D. Guerrero¹⁸⁴, B. M. Joshi¹⁸⁴, M. Kim¹⁸⁴, E. Koenig¹⁸⁴, J. Konigsberg¹⁸⁴, A. Korytov¹⁸⁴, K. H. Lo¹⁸⁴, K. Matchev¹⁸⁴, N. Menendez¹⁸⁴, G. Mitselmakher¹⁸⁴, A. Muthirakalayil Madhu¹⁸⁴, N. Rawal¹⁸⁴, D. Rosenzweig¹⁸⁴, S. Rosenzweig¹⁸⁴, J. Rotter¹⁸⁴, K. Shi¹⁸⁴, J. Wang¹⁸⁴, E. Yigitbasi¹⁸⁴, X. Zuo¹⁸⁴, T. Adams¹⁸⁵, A. Askew¹⁸⁵, R. Habibullah¹⁸⁵, V. Hagopian¹⁸⁵, K. F. Johnson¹⁸⁵, R. Khurana¹⁸⁵, T. Kolberg¹⁸⁵, G. Martinez¹⁸⁵, H. Prosper¹⁸⁵, C. Schiber¹⁸⁵, O. Viazlo¹⁸⁵, R. Yohay¹⁸⁵, J. Zhang¹⁸⁵, M. M. Baarmand¹⁸⁶, S. Butalla¹⁸⁶, T. Elkafrawy^{186,31}, M. Hohlmann¹⁸⁶, R. Kumar Verma¹⁸⁶, D. Noonan¹⁸⁶, M. Rahmani¹⁸⁶, F. Yumiceva¹⁸⁶, M. R. Adams¹⁸⁷, H. Becerril Gonzalez¹⁸⁷, R. Cavanaugh¹⁸⁷, S. Dittmer¹⁸⁷, O. Evdokimov¹⁸⁷, C. E. Gerber¹⁸⁷, D. A. Hangal¹⁸⁷, D. J. Hofman¹⁸⁷, A. H. Merrit¹⁸⁷, C. Mills¹⁸⁷, G. Oh¹⁸⁷, T. Roy¹⁸⁷, S. Rudrabhatla¹⁸⁷, M. B. Tonjes¹⁸⁷, N. Varelas¹⁸⁷, J. Viinikainen¹⁸⁷, X. Wang¹⁸⁷, Z. Wu¹⁸⁷, Z. Ye¹⁸⁷, M. Alhusseini¹⁸⁸, K. Dilsiz^{188,309}, L. Emediato¹⁸⁸, R. P. Gandrajula¹⁸⁸, O. K. Köseyan¹⁸⁸, J.-P. Merlo¹⁸⁸, A. Mestvirishvili^{188,310}, J. Nachtman¹⁸⁸, H. Ogul^{188,311}, Y. Onel¹⁸⁸, A. Penzo¹⁸⁸, C. Snyder¹⁸⁸, E. Tiras^{188,312}, O. Amram¹⁸⁹, B. Blumenfeld¹⁸⁹, L. Corcodilos¹⁸⁹, J. Davis¹⁸⁹, M. Eminizer¹⁸⁹, A. V. Gritsan¹⁸⁹, S. Kyriacou¹⁸⁹, P. Maksimovic¹⁸⁹, J. Roskes¹⁸⁹, M. Swartz¹⁸⁹, T.Á. Vámi¹⁸⁹, A. Abreu¹⁹⁰, J. Anguiano¹⁹⁰, C. Baldenegro Barrera¹⁹⁰, P. Baringer¹⁹⁰, A. Bean¹⁹⁰, A. Bylinkin¹⁹⁰, Z. Flowers¹⁹⁰, T. Isidori¹⁹⁰, S. Khalil¹⁹⁰, J. King¹⁹⁰, G. Krintiras¹⁹⁰, A. Kropivnitskaya¹⁹⁰, M. Lazarovits¹⁹⁰, C. Le Mahieu¹⁹⁰, C. Lindsey¹⁹⁰, J. Marquez¹⁹⁰, M. Minafra¹⁹⁰, M. Murray¹⁹⁰, M. Nickel¹⁹⁰, C. Rogan¹⁹⁰, C. Royon¹⁹⁰, R. Salvatico¹⁹⁰, S. Sanders¹⁹⁰, E. Schmitz¹⁹⁰, C. Smith¹⁹⁰, J. D. Tapia Takaki¹⁹⁰, Q. Wang¹⁹⁰, Z. Warner¹⁹⁰, J. Williams¹⁹⁰, G. Wilson¹⁹⁰, S. Duric¹⁹¹, A. Ivanov¹⁹¹, K. Kaadze¹⁹¹, D. Kim¹⁹¹, Y. Maravin¹⁹¹, T. Mitchell¹⁹¹, A. Modak¹⁹¹, K. Nam¹⁹¹, F. Rebassoo¹⁹², D. Wright¹⁹², E. Adams¹⁹³, A. Baden¹⁹³, O. Baron¹⁹³, A. Belloni¹⁹³, S. C. Eno¹⁹³, N. J. Hadley¹⁹³, S. Jabeen¹⁹³, R. G. Kellogg¹⁹³, T. Koeth¹⁹³, Y. Lai¹⁹³, S. Lascio¹⁹³, A. C. Mignerey¹⁹³, S. Nabili¹⁹³, C. Palmer¹⁹³, M. Seidel¹⁹³, A. Skuja¹⁹³, L. Wang¹⁹³, K. Wong¹⁹³, D. Abercrombie¹⁹⁴, G. Andreassi¹⁹⁴, R. Bi¹⁹⁴, W. Busza¹⁹⁴, I. A. Calì¹⁹⁴, Y. Chen¹⁹⁴, M. D'Alfonso¹⁹⁴, J. Eysermans¹⁹⁴, C. Freer¹⁹⁴, G. Gomez Ceballos¹⁹⁴, M. Goncharov¹⁹⁴, P. Harris¹⁹⁴, M. Hu¹⁹⁴, M. Klute¹⁹⁴, D. Kovalskyi¹⁹⁴, J. Krupa¹⁹⁴, Y.-J. Lee¹⁹⁴, C. Mironov¹⁹⁴, C. Paus¹⁹⁴, D. Rankin¹⁹⁴, C. Roland¹⁹⁴, G. Roland¹⁹⁴, Z. Shi¹⁹⁴, G. S. F. Stephens¹⁹⁴, J. Wang¹⁹⁴, Z. Wang¹⁹⁴, B. Wyslouch¹⁹⁴, R. M. Chatterjee¹⁹⁵, A. Evans¹⁹⁵, J. Hiltbrand¹⁹⁵, Sh. Jain¹⁹⁵, M. Krohn¹⁹⁵, Y. Kubota¹⁹⁵, J. Mans¹⁹⁵, M. Revering¹⁹⁵, R. Rusack¹⁹⁵, R. Saradhy¹⁹⁵, N. Schroeder¹⁹⁵, N. Strobbe¹⁹⁵, M. A. Wadud¹⁹⁵, K. Bloom¹⁹⁶, M. Bryson¹⁹⁶, S. Chauhan¹⁹⁶, D. R. Claes¹⁹⁶, C. Fangmeier¹⁹⁶, L. Finco¹⁹⁶, F. Golf¹⁹⁶, C. Joo¹⁹⁶, I. Kravchenko¹⁹⁶, M. Musich¹⁹⁶, I. Reed¹⁹⁶, J. E. Siado¹⁹⁶, G. R. Snow^{196,318}, W. Tabb¹⁹⁶, F. Yan¹⁹⁶, A. G. Zecchinelli¹⁹⁶, G. Agarwal¹⁹⁷, H. Bandyopadhyay¹⁹⁷, L. Hay¹⁹⁷, I. Iashvili¹⁹⁷, A. Kharchilava¹⁹⁷, C. McLean¹⁹⁷, D. Nguyen¹⁹⁷, J. Pekkanen¹⁹⁷, S. Rappoccio¹⁹⁷, A. Williams¹⁹⁷, G. Alverson¹⁹⁸, E. Barberis¹⁹⁸, Y. Haddad¹⁹⁸, Y. Han¹⁹⁸, A. Hortiangtham¹⁹⁸, A. Krishna¹⁹⁸, J. Li¹⁹⁸, G. Madigan¹⁹⁸, B. Marzocchi¹⁹⁸, D. M. Morse¹⁹⁸, V. Nguyen¹⁹⁸, T. Orimoto¹⁹⁸, A. Parker¹⁹⁸, L. Skinnari¹⁹⁸, A. Tishelman-Charny¹⁹⁸, T. Wamorkar¹⁹⁸, B. Wang¹⁹⁸, A. Wisecarver¹⁹⁸, D. Wood¹⁹⁸, S. Bhattacharya¹⁹⁹, J. Bueghly¹⁹⁹, Z. Chen¹⁹⁹, A. Gilbert¹⁹⁹, T. Gunter¹⁹⁹, K. A. Hahn¹⁹⁹, Y. Liu¹⁹⁹, N. Odell¹⁹⁹, M. H. Schmitt¹⁹⁹, M. Velasco¹⁹⁹, R. Band²⁰⁰, R. Bucci²⁰⁰, M. Cremonesi²⁰⁰, A. Das²⁰⁰, N. Dev²⁰⁰, R. Goldouzian²⁰⁰, M. Hildreth²⁰⁰, K. Hurtado Anampa²⁰⁰, C. Jessop²⁰⁰, K. Lannon²⁰⁰, J. Lawrence²⁰⁰, N. Loukas²⁰⁰, D. Lutton²⁰⁰, J. Mariano²⁰⁰, N. Marinelli²⁰⁰, I. Mcalister²⁰⁰, T. McCauley²⁰⁰, C. Mcgrady²⁰⁰, K. Mohrman²⁰⁰, C. Moore²⁰⁰, Y. Musienko^{200,269}, R. Ruchti²⁰⁰, A. Townsend²⁰⁰, M. Wayne²⁰⁰, A. Wightman²⁰⁰, M. Zarucki²⁰⁰, L. Zygala²⁰⁰, B. Bylsma²⁰¹, L. S. Durkin²⁰¹, B. Francis²⁰¹, C. Hill²⁰¹, M. Nunez Ornelas²⁰¹, K. Wei²⁰¹, B. L. Winer²⁰¹, B. R. Yates²⁰¹, F. M. Addesa²⁰², B. Bonham²⁰², P. Das²⁰², G. Dezoort²⁰², P. Elmer²⁰², A. Frankenthal²⁰², B. Greenberg²⁰², N. Haubrich²⁰², S. Higginbotham²⁰², A. Kalogeropoulos²⁰², G. Kopp²⁰², S. Kwan²⁰², D. Lange²⁰², D. Marlow²⁰², K. Mei²⁰², I. Ojalvo²⁰², J. Olsen²⁰², D. Stickland²⁰², C. Tully²⁰², S. Malik²⁰³, S. Norberg²⁰³, A. S. Bakshi²⁰⁴, V. E. Barnes²⁰⁴, R. Chawla²⁰⁴, S. Das²⁰⁴, L. Gutay²⁰⁴, M. Jones²⁰⁴, A. W. Jung²⁰⁴, S. Karmarkar²⁰⁴, D. Kondratyev²⁰⁴, A. M. Koshy²⁰⁴, M. Liu²⁰⁴, G. Negro²⁰⁴, N. Neumeister²⁰⁴, G. Paspalaki²⁰⁴, S. Piperov²⁰⁴, A. Purohit²⁰⁴, J. F. Schulte²⁰⁴, M. Stojanovic^{204,232}, J. Thieman²⁰⁴, F. Wang²⁰⁴, R. Xiao²⁰⁴, W. Xie²⁰⁴, J. Dolen²⁰⁵, N. Parashar²⁰⁵, A. Baty²⁰⁶, T. Carnahan²⁰⁶, M. Decaro²⁰⁶, S. Dildick²⁰⁶, K. M. Ecklund²⁰⁶, S. Freed²⁰⁶, P. Gardner²⁰⁶, F.J.M. Geurts²⁰⁶, A. Kumar²⁰⁶, W. Li²⁰⁶, B. P. Padley²⁰⁶, R. Redjimi²⁰⁶, W. Shi²⁰⁶, A. G. Stahl Leitner²⁰⁶, S. Yang²⁰⁶, L. Zhang^{206,313}, Y. Zhang²⁰⁶, A. Bodek²⁰⁷, P. de Barbaro²⁰⁷, R. Demina²⁰⁷, J. L. Dulemba²⁰⁷, C. Fallon²⁰⁷, T. Ferbel²⁰⁷, M. Galanti²⁰⁷, A. Garcia-Bellido²⁰⁷, O. Hindrichs²⁰⁷, A. Khukhunaishvili²⁰⁷, E. Ranken²⁰⁷, R. Taus²⁰⁷, B. Chiarito²⁰⁸, J. P. Chou²⁰⁸, A. Gandrakota²⁰⁸, Y. Gershtein²⁰⁸, E. Halkiadakis²⁰⁸, A. Hart²⁰⁸, M. Heindl²⁰⁸, O. Karacheban^{208,240}, I. Laflotte²⁰⁸, A. Lath²⁰⁸, R. Montalvo²⁰⁸, K. Nash²⁰⁸, M. Osherson²⁰⁸, S. Salur²⁰⁸, S. Schnetzer²⁰⁸, S. Somalwar²⁰⁸, R. Stone²⁰⁸, S. A. Thayil²⁰⁸, S. Thomas²⁰⁸, H. Wang²⁰⁸, H. Acharya²⁰⁹, A. G. Delannoy²⁰⁹, S. Fiorendi²⁰⁹, S. Spanier²⁰⁹, O. Bouhali^{210,314}, M. Dalchenko²¹⁰, A. Delgado²¹⁰, R. Eusebi²¹⁰, J. Gilmore²¹⁰, T. Huang²¹⁰, T. Kamon^{210,315}, H. Kim²¹⁰, S. Luo²¹⁰, S. Malhotra²¹⁰, R. Mueller²¹⁰, D. Overton²¹⁰, D. Rathjens²¹⁰, A. Safonov²¹⁰, N. Akchurin²¹¹, J. Damgov²¹¹, V. Hegde²¹¹, S. Kunori²¹¹, K. Lamichhane²¹¹, S. W. Lee²¹¹, T. Mengke²¹¹, S. Muthumuni²¹¹, T. Peltola²¹¹, I. Volobouev²¹¹, Z. Wang²¹¹, A. Whitbeck²¹¹, E. Appelt²¹², S. Greene²¹², A. Gurrola²¹², W. Johns²¹², A. Melo²¹², H. Ni²¹², K. Padeken²¹², F. Romeo²¹², P. Sheldon²¹², S. Tuo²¹², J. Velkovska²¹², M. W. Arenton²¹³, B. Cardwell²¹³, B. Cox²¹³, G. Cummings²¹³, J. Hakala²¹³, R. Hirosky²¹³, M. Joyce²¹³, A. Ledovskoy²¹³, A. Li²¹³, C. Neu²¹³, C. E. Perez Lara²¹³, B. Tannenwald²¹³, S. White²¹³, N. Poudyal²¹⁴, S. Banerjee²¹⁵, K. Black²¹⁵, T. Bose²¹⁵, S. Dasu²¹⁵, I. De Bruyn²¹⁵, P. Everaerts²¹⁵, C. Galloni²¹⁵, H. He²¹⁵, M. Herndon²¹⁵, A. Hervé²¹⁵, U. Hussain²¹⁵, A. Lanaro²¹⁵, A. Loeliger²¹⁵, R. Loveless²¹⁵, J. Madhusudanan Sreekala²¹⁵, A. Mallampalli²¹⁵, A. Mohammadi²¹⁵, D. Pinna²¹⁵, A. Savin²¹⁵, V. Shang²¹⁵, V. Sharma²¹⁵, W. H. Smith²¹⁵, D. Teague²¹⁵, S. Trembath-Reichert²¹⁵ & W. Vetens²¹⁵

¹Yerevan Physics Institute, Yerevan, Armenia. ²Institut für Hochenergiephysik, Vienna, Austria. ³Institute for Nuclear Problems, Minsk, Belarus. ⁴Universiteit Antwerpen, Antwerpen, Belgium. ⁵Vrije Universiteit Brussel, Brussel, Belgium. ⁶Université Libre de Bruxelles, Bruxelles, Belgium. ⁷Ghent University, Ghent, Belgium. ⁸Université Catholique de Louvain, Louvain-la-Neuve, Belgium. ⁹Centro Brasileiro de Pesquisas Físicas, Rio de Janeiro, Brazil. ¹⁰Universidade do Estado do Rio de Janeiro, Rio de Janeiro, Brazil. ¹¹Universidade Estadual Paulista, São Paulo, Brazil. ¹²Universidade Federal do ABC, São Paulo, Brazil. ¹³Institute for Nuclear Research and Nuclear Energy, Bulgarian Academy of Sciences, Sofia, Bulgaria. ¹⁴University of Sofia, Sofia, Bulgaria. ¹⁵Beihang University, Beijing, China. ¹⁶Department of Physics, Tsinghua University, Beijing, China. ¹⁷Institute of High Energy Physics, Beijing, China. ¹⁸State Key Laboratory of Nuclear Physics and Technology, Peking University, Beijing, China. ¹⁹Sun Yat-Sen University, Guangzhou, China. ²⁰Institute of Modern Physics and Key Laboratory of Nuclear Physics and Ion-beam Application (MOE) - Fudan University, Shanghai, China. ²¹Zhejiang University, Hangzhou, China, Zhejiang, China. ²²Universidad de Los Andes, Bogota, Colombia. ²³Universidad de Antioquia, Medellin, Colombia. ²⁴University of Split, Faculty of Electrical Engineering, Mechanical Engineering and Naval Architecture, Split, Croatia. ²⁵University of Split, Faculty of Science, Split, Croatia.

²⁶Institute Rudjer Boskovic, Zagreb, Croatia. ²⁷University of Cyprus, Nicosia, Cyprus. ²⁸Charles University, Prague, Czech Republic. ²⁹Escuela Politecnica Nacional, Quito, Ecuador. ³⁰Universidad San Francisco de Quito, Quito, Ecuador. ³¹Academy of Scientific Research and Technology of the Arab Republic of Egypt, Egyptian Network of High Energy Physics, Cairo, Egypt. ³²Center for High Energy Physics (CHEP-FU), Fayoum University, El-Fayoum, Egypt. ³³National Institute of Chemical Physics and Biophysics, Tallinn, Estonia. ³⁴Department of Physics, University of Helsinki, Helsinki, Finland. ³⁵Helsinki Institute of Physics, Helsinki, Finland. ³⁶Lappeenranta University of Technology, Lappeenranta, Finland. ³⁷IRFU, CEA, Université Paris-Saclay, Gif-sur-Yvette, France. ³⁸Laboratoire Leprince-Ringuet, CNRS/IN2P3, Ecole Polytechnique, Institut Polytechnique de Paris, Palaiseau, France. ³⁹Université de Strasbourg, CNRS, IPHC UMR 7178, Strasbourg, France. ⁴⁰Institut de Physique des 2 Infinis de Lyon (IP2I), Villeurbanne, France. ⁴¹Georgian Technical University, Tbilisi, Georgia. ⁴²RWTH Aachen University, I. Physikalisches Institut, Aachen, Germany. ⁴³RWTH Aachen University, III. Physikalisches Institut A, Aachen, Germany. ⁴⁴RWTH Aachen University, III. Physikalisches Institut B, Aachen, Germany. ⁴⁵Deutsches Elektronen-Synchrotron, Hamburg, Germany. ⁴⁶University of Hamburg, Hamburg, Germany. ⁴⁷Karlsruher Institut fuer Technologie, Karlsruhe, Germany. ⁴⁸Institute of Nuclear and Particle Physics (INPP), NCSR Demokritos, Aghia Paraskevi, Greece. ⁴⁹National and Kapodistrian University of Athens, Athens, Greece. ⁵⁰National Technical University of Athens, Athens, Greece. ⁵¹University of Ioánnina, Ioánnina, Greece. ⁵²MTA-ELTE Lendület CMS Particle and Nuclear Physics Group, Eötvös Loránd University, Budapest, Hungary. ⁵³Wigner Research Centre for Physics, Budapest, Hungary. ⁵⁴Institute of Nuclear Research ATOMKI, Debrecen, Hungary. ⁵⁵Institute of Physics, University of Debrecen, Debrecen, Hungary. ⁵⁶Karoly Robert Campus, MATE Institute of Technology, Gyongyos, Hungary. ⁵⁷Indian Institute of Science (IISc), Bangalore, India. ⁵⁸National Institute of Science Education and Research, HBNI, Bhubaneswar, India. ⁵⁹Panjab University, Chandigarh, India. ⁶⁰University of Delhi, Delhi, India. ⁶¹Saha Institute of Nuclear Physics, HBNI, Kolkata, India. ⁶²Indian Institute of Technology Madras, Madras, India. ⁶³Bhabha Atomic Research Centre, Mumbai, India. ⁶⁴Tata Institute of Fundamental Research-A, Mumbai, India. ⁶⁵Tata Institute of Fundamental Research-B, Mumbai, India. ⁶⁶Indian Institute of Science Education and Research (IISER), Pune, India. ⁶⁷Isfahan University of Technology, Isfahan, Iran. ⁶⁸Institute for Research in Fundamental Sciences (IPM), Tehran, Iran. ⁶⁹University College Dublin, Dublin, Ireland. ⁷⁰INFN Sezione di Bari, Bari, Italy. ⁷¹Università di Bari, Bari, Italy. ⁷²Politecnico di Bari, Bari, Italy. ⁷³INFN Sezione di Bologna, Bologna, Italy. ⁷⁴Università di Bologna, Bologna, Italy. ⁷⁵INFN Sezione di Catania, Catania, Italy. ⁷⁶Università di Catania, Catania, Italy. ⁷⁷INFN Sezione di Firenze, Firenze, Italy. ⁷⁸Università di Firenze, Firenze, Italy. ⁷⁹INFN Laboratori Nazionali di Frascati, Frascati, Italy. ⁸⁰INFN Sezione di Genova, Genova, Italy. ⁸¹Università di Genova, Genova, Italy. ⁸²INFN Sezione di Milano-Bicocca, Milano, Italy. ⁸³Università di Milano-Bicocca, Milano, Italy. ⁸⁴INFN Sezione di Napoli, Napoli, Italy. ⁸⁵Università di Napoli 'Federico II', Napoli, Italy. ⁸⁶Università della Basilicata, Potenza, Italy. ⁸⁷Università G. Marconi, Roma, Italy. ⁸⁸INFN Sezione di Padova, Padova, Italy. ⁸⁹Università di Padova, Padova, Italy. ⁹⁰Università di Trento, Trento, Italy. ⁹¹INFN Sezione di Pavia, Pavia, Italy. ⁹²Università di Pavia, Pavia, Italy. ⁹³INFN Sezione di Perugia, Perugia, Italy. ⁹⁴Università di Perugia, Perugia, Italy. ⁹⁵INFN Sezione di Pisa, Pisa, Italy. ⁹⁶Scuola Normale Superiore di Pisa, Pisa, Italy. ⁹⁷Università di Pisa, Pisa, Italy. ⁹⁸Università di Siena, Siena, Italy. ⁹⁹INFN Sezione di Roma, Rome, Italy. ¹⁰⁰Sapienza Università di Roma, Rome, Italy. ¹⁰¹INFN Sezione di Torino, Torino, Italy. ¹⁰²Università di Torino, Torino, Italy. ¹⁰³Università del Piemonte Orientale, Novara, Italy. ¹⁰⁴INFN Sezione di Trieste, Trieste, Italy. ¹⁰⁵Università di Trieste, Trieste, Italy. ¹⁰⁶Kyungpook National University, Daegu, Korea. ¹⁰⁷Chonnam National University, Institute for Universe and Elementary Particles, Kwangju, Korea. ¹⁰⁸Hanyang University, Seoul, Korea. ¹⁰⁹Korea University, Seoul, Korea. ¹¹⁰Kyung Hee University, Department of Physics, Seoul, Republic of Korea, Seoul, Korea. ¹¹¹Sejong University, Seoul, Korea. ¹¹²Seoul National University, Seoul, Korea. ¹¹³University of Seoul, Seoul, Korea. ¹¹⁴Yonsei University, Department of Physics, Seoul, Korea. ¹¹⁵Sungkyunkwan University, Suwon, Korea. ¹¹⁶College of Engineering and Technology, American University of the Middle East (AUM), Egaila, Kuwait, Dasman, Kuwait. ¹¹⁷Riga Technical University, Riga, Latvia. ¹¹⁸Vilnius University, Vilnius, Lithuania. ¹¹⁹National Centre for Particle Physics, Universiti Malaya, Kuala Lumpur, Malaysia. ¹²⁰Universidad de Sonora (UNISON), Hermosillo, Mexico. ¹²¹Centro de Investigacion y de Estudios Avanzados del IPN, Mexico City, Mexico. ¹²²Universidad Iberoamericana, Mexico City, Mexico. ¹²³Benemerita Universidad Autonoma de Puebla, Puebla, Mexico. ¹²⁴University of Montenegro, Podgorica, Montenegro. ¹²⁵University of Auckland, Auckland, New Zealand. ¹²⁶University of Canterbury, Christchurch, New Zealand. ¹²⁷National Centre for Physics, Quaid-I-Azam University, Islamabad, Pakistan. ¹²⁸AGH University of Science and Technology Faculty of Computer Science, Electronics and Telecommunications, Krakow, Poland. ¹²⁹National Centre for Nuclear Research, Swierk, Poland. ¹³⁰Institute of Experimental Physics, Faculty of Physics, University of Warsaw, Warsaw, Poland. ¹³¹Laboratório de Instrumentação e Física Experimental de Partículas, Lisboa, Portugal. ¹³²Joint Institute for Nuclear Research, Dubna, Russia. ¹³³Petersburg Nuclear Physics Institute, Gatchina (St. Petersburg), Russia. ¹³⁴Institute for Nuclear Research, Moscow, Russia. ¹³⁵Institute for Theoretical and Experimental Physics named by A.I. Alikhanov of NRC 'Kurchatov Institute', Moscow, Russia. ¹³⁶Moscow Institute of Physics and Technology, Moscow, Russia. ¹³⁷National Research Nuclear University 'Moscow Engineering Physics Institute' (MEPhI), Moscow, Russia. ¹³⁸P.N. Lebedev Physical Institute, Moscow, Russia. ¹³⁹Skobeltsyn Institute of Nuclear Physics, Lomonosov Moscow State University, Moscow, Russia. ¹⁴⁰Novosibirsk State University (NSU), Novosibirsk, Russia. ¹⁴¹Institute for High Energy Physics of National Research Centre 'Kurchatov Institute', Protvino, Russia. ¹⁴²National Research Tomsk Polytechnic University, Tomsk, Russia. ¹⁴³Tomsk State University, Tomsk, Russia. ¹⁴⁴University of Belgrade: Faculty of Physics and VINCA Institute of Nuclear Sciences, Belgrade, Serbia. ¹⁴⁵Centro de Investigaciones Energéticas Medioambientales y Tecnológicas (CIEMAT), Madrid, Spain. ¹⁴⁶Universidad Autónoma de Madrid, Madrid, Spain. ¹⁴⁷Universidad de Oviedo, Instituto Universitario de Ciencias y Tecnologías Espaciales de Asturias (ICTEA), Oviedo, Spain. ¹⁴⁸Instituto de Física de Cantabria (IFCA), CSIC-Universidad de Cantabria, Santander, Spain. ¹⁴⁹University of Colombo, Colombo, Sri Lanka. ¹⁵⁰University of Ruhuna, Department of Physics, Matara, Sri Lanka. ¹⁵¹CERN, European Organization for Nuclear Research, Geneva, Switzerland. ¹⁵²Paul Scherrer Institut, Villigen, Switzerland. ¹⁵³ETH Zurich - Institute for Particle Physics and Astrophysics (IPA), Zurich, Switzerland. ¹⁵⁴Universität Zürich, Zurich, Switzerland. ¹⁵⁵National Central University, Chung-Li, Taiwan. ¹⁵⁶National Taiwan University (NTU), Taipei, Taiwan. ¹⁵⁷Chulalongkorn University, Faculty of Science, Department of Physics, Bangkok, Thailand. ¹⁵⁸Çukurova University, Physics Department, Science and Art Faculty, Adana, Turkey. ¹⁵⁹Middle East Technical University, Physics Department, Ankara, Turkey. ¹⁶⁰Bogazici University, Istanbul, Turkey. ¹⁶¹Istanbul Technical University, Istanbul, Turkey. ¹⁶²Istanbul University, Istanbul, Turkey. ¹⁶³Institute for Scintillation Materials of National Academy of Science of Ukraine, Kharkov, Ukraine. ¹⁶⁴National Scientific Center, Kharkov Institute of Physics and Technology, Kharkov, Ukraine. ¹⁶⁵University of Bristol, Bristol, United Kingdom. ¹⁶⁶Rutherford Appleton Laboratory, Didcot, United Kingdom. ¹⁶⁷Imperial College, London, United Kingdom. ¹⁶⁸Brunel University, Uxbridge, United Kingdom. ¹⁶⁹Baylor University, Waco, Texas, USA. ¹⁷⁰Catholic University of America, Washington, DC, USA. ¹⁷¹The University of Alabama, Tuscaloosa, Alabama, USA. ¹⁷²Boston University, Boston, Massachusetts, USA. ¹⁷³Brown University, Providence, Rhode Island, USA. ¹⁷⁴University of California, Davis, Davis, California, USA. ¹⁷⁵University of California, Los Angeles, California, USA. ¹⁷⁶University of California, Riverside, Riverside, California, USA. ¹⁷⁷University of California, San Diego, La Jolla, California, USA. ¹⁷⁸University of California, Santa Barbara - Department of Physics, Santa Barbara, California, USA. ¹⁷⁹California Institute of Technology, Pasadena, California, USA. ¹⁸⁰Carnegie Mellon University, Pittsburgh, Pennsylvania, USA. ¹⁸¹University of Colorado Boulder, Boulder, Colorado, USA. ¹⁸²Cornell University, Ithaca, New York, USA. ¹⁸³Fermi National Accelerator Laboratory, Batavia, Illinois, USA. ¹⁸⁴University of Florida, Gainesville, Florida, USA. ¹⁸⁵Florida State University, Tallahassee, Florida, USA. ¹⁸⁶Florida Institute of Technology, Melbourne, Florida, USA. ¹⁸⁷University of Illinois at Chicago (UIC), Chicago, Illinois, USA. ¹⁸⁸The University of Iowa, Iowa City, Iowa, USA. ¹⁸⁹Johns Hopkins University, Baltimore, Maryland, USA. ¹⁹⁰The University of Kansas, Lawrence, Kansas, USA. ¹⁹¹Kansas State University, Manhattan, Kansas, USA. ¹⁹²Lawrence Livermore

National Laboratory, Livermore, California, USA. ¹⁹³University of Maryland, College Park, Maryland, USA. ¹⁹⁴Massachusetts Institute of Technology, Cambridge, Massachusetts, USA. ¹⁹⁵University of Minnesota, Minneapolis, Minnesota, USA. ¹⁹⁶University of Nebraska-Lincoln, Lincoln, Nebraska, USA. ¹⁹⁷State University of New York at Buffalo, Buffalo, New York, USA. ¹⁹⁸Northeastern University, Boston, Massachusetts, USA. ¹⁹⁹Northwestern University, Evanston, Illinois, USA. ²⁰⁰University of Notre Dame, Notre Dame, Indiana, USA. ²⁰¹The Ohio State University, Columbus, Ohio, USA. ²⁰²Princeton University, Princeton, New Jersey, USA. ²⁰³University of Puerto Rico, Mayaguez, Puerto Rico, USA. ²⁰⁴Purdue University, West Lafayette, Indiana, USA. ²⁰⁵Purdue University Northwest, Hammond, Indiana, USA. ²⁰⁶Rice University, Houston, Texas, USA. ²⁰⁷University of Rochester, Rochester, New York, USA. ²⁰⁸Rutgers, The State University of New Jersey, Piscataway, New Jersey, USA. ²⁰⁹University of Tennessee, Knoxville, Tennessee, USA. ²¹⁰Texas A&M University, College Station, Texas, USA. ²¹¹Texas Tech University, Lubbock, Texas, USA. ²¹²Vanderbilt University, Nashville, Tennessee, USA. ²¹³University of Virginia, Charlottesville, Virginia, USA. ²¹⁴Wayne State University, Detroit, Michigan, USA. ²¹⁵University of Wisconsin - Madison, Madison, WI, Wisconsin, USA. ²¹⁶Present address: TU Wien, Wien, Austria. ²¹⁷Present address: Institute of Basic and Applied Sciences, Faculty of Engineering, Arab Academy for Science, Technology and Maritime Transport, Alexandria, Egypt. ²¹⁸Present address: Université Libre de Bruxelles, Bruxelles, Belgium. ²¹⁹Present address: Universidade Estadual de Campinas, Campinas, Brazil. ²²⁰Present address: Federal University of Rio Grande do Sul, Porto Alegre, Brazil. ²²¹Present address: The University of the State of Amazonas, Manaus, Brazil. ²²²Present address: University of Chinese Academy of Sciences, Beijing, China. ²²³Present address: Department of Physics, Tsinghua University, Beijing, China. ²²⁴Present address: UFMS, Nova Andradina, Brazil. ²²⁵Present address: Nanjing Normal University Department of Physics, Nanjing, China. ²²⁶Present address: The University of Iowa, Iowa City, Iowa, USA. ²²⁷Present address: Institute for Theoretical and Experimental Physics named by A.I. Alikhanov of NRC 'Kurchatov Institute', Moscow, Russia. ²²⁸Present address: Joint Institute for Nuclear Research, Dubna, Russia. ²²⁹Present address: Helwan University, Cairo, Egypt. ²³⁰Present address: Zewail City of Science and Technology, Zewail, Egypt. ²³¹Ain Shams University, Cairo, Egypt. ²³²Present address: Purdue University, West Lafayette, Indiana, USA. ²³³Present address: Université de Haute Alsace, Mulhouse, France. ²³⁴Present address: Tbilisi State University, Tbilisi, Georgia. ²³⁵Present address: Erzincan Binali Yildirim University, Erzincan, Turkey. ²³⁶Present address: CERN, European Organization for Nuclear Research, Geneva, Switzerland. ²³⁷Present address: RWTH Aachen University, III. Physikalisches Institut A, Aachen, Germany. ²³⁸Present address: University of Hamburg, Hamburg, Germany. ²³⁹Present address: Isfahan University of Technology, Isfahan, Iran. ²⁴⁰Present address: Brandenburg University of Technology, Cottbus, Germany. ²⁴¹Present address: Forschungszentrum Jülich, Jülich, Germany. ²⁴²Present address: Physics Department, Faculty of Science, Assiut University, Assiut, Egypt. ²⁴³Present address: Karoly Robert Campus, MATE Institute of Technology, Gyongyos, Hungary. ²⁴⁴Present address: Institute of Physics, University of Debrecen, Debrecen, Hungary. ²⁴⁵Present address: Institute of Nuclear Research ATOMKI, Debrecen, Hungary. ²⁴⁶Present address: MTA-ELTE Lendület CMS Particle and Nuclear Physics Group, Eötvös Loránd University, Budapest, Hungary. ²⁴⁷Present address: Wigner Research Centre for Physics, Budapest, Hungary. ²⁴⁸Present address: IIT Bhubaneswar, Bhubaneswar, India. ²⁴⁹Present address: Institute of Physics, Bhubaneswar, India. ²⁵⁰Present address: Punjab Agricultural University, Ludhiana, India. ²⁵¹Present address: Shoolini University, Solan, India. ²⁵²Present address: University of Hyderabad, Hyderabad, India. ²⁵³Present address: University of Visva-Bharati, Santiniketan, India. ²⁵⁴Present address: Indian Institute of Technology (IIT), Mumbai, India. ²⁵⁵Present address: Deutsches Elektronen-Synchrotron, Hamburg, Germany. ²⁵⁶Present address: Sharif University of Technology, Tehran, Iran. ²⁵⁷Present address: Department of Physics, University of Science and Technology of Mazandaran, Behshahr, Iran. ²⁵⁸Present address: INFN Sezione di Bari, Bari, Italy. ²⁵⁹Present address: Università di Bari, Bari, Italy. ²⁶⁰Present address: Politecnico di Bari, Bari, Italy. ²⁶¹Present address: Italian National Agency for New Technologies, Energy and Sustainable Economic Development, Bologna, Italy. ²⁶²Present address: Centro Siciliano di Fisica Nucleare e di Struttura Della Materia, Catania, Italy. ²⁶³Present address: Scuola Superiore Meridionale, Università di Napoli Federico II, Napoli, Italy. ²⁶⁴Present address: Università di Napoli 'Federico II', Napoli, Italy. ²⁶⁵Present address: Consiglio Nazionale delle Ricerche - Istituto Officina dei Materiali, Perugia, Italy. ²⁶⁶Present address: Riga Technical University, Riga, Latvia. ²⁶⁷Present address: Consejo Nacional de Ciencia y Tecnología, Mexico City, Mexico. ²⁶⁸Present address: IRFU, CEA, Université Paris-Saclay, Gif-sur-Yvette, France. ²⁶⁹Present address: Institute for Nuclear Research, Moscow, Russia. ²⁷⁰Present address: National Research Nuclear University "Moscow Engineering Physics Institute" (MEPhI), Moscow, Russia. ²⁷¹Present address: Institute of Nuclear Physics of the Uzbekistan Academy of Sciences, Tashkent, Uzbekistan. ²⁷²Present address: St. Petersburg State Polytechnical University, St. Petersburg, Russia. ²⁷³Present address: University of Florida, Gainesville, Florida, USA. ²⁷⁴Present address: Imperial College, London, United Kingdom. ²⁷⁵Present address: P.N. Lebedev Physical Institute, Moscow, Russia. ²⁷⁶Present address: California Institute of Technology, Pasadena, California, USA. ²⁷⁷Present address: Budker Institute of Nuclear Physics, Novosibirsk, Russia. ²⁷⁸Present address: Faculty of Physics, University of Belgrade, Belgrade, Serbia. ²⁷⁹Present address: Trincomalee Campus, Eastern University, Sri Lanka, Nilaveli, Sri Lanka. ²⁸⁰Present address: INFN Sezione di Pavia, Pavia, Italy. ²⁸¹Present address: Università di Pavia, Pavia, Italy. ²⁸²Present address: National and Kapodistrian University of Athens, Athens, Greece. ²⁸³Present address: Ecole Polytechnique Fédérale Lausanne, Lausanne, Switzerland. ²⁸⁴Present address: Universität Zürich, Zurich, Switzerland. ²⁸⁵Present address: Stefan Meyer Institute for Subatomic Physics, Vienna, Austria. ²⁸⁶Present address: Laboratoire d'Annecy-le-Vieux de Physique des Particules, IN2P3-CNRS, Annecy-le-Vieux, France. ²⁸⁷Present address: rnak University, Sirkak, Turkey. ²⁸⁸Present address: Near East University, Research Center of Experimental Health Science, Nicosia, Turkey. ²⁸⁹Present address: Konya Technical University, Konya, Turkey. ²⁹⁰Present address: Piri Reis University, Istanbul, Turkey. ²⁹¹Present address: Adiyaman University, Adiyaman, Turkey. ²⁹²Present address: Ozyegin University, Istanbul, Turkey. ²⁹³Present address: Necmettin Erbakan University, Konya, Turkey. ²⁹⁴Present address: Bozok Universiteleri Rektörlüğü, Yozgat, Turkey. ²⁹⁵Present address: Marmara University, Istanbul, Turkey. ²⁹⁶Present address: Milli Savunma University, Istanbul, Turkey. ²⁹⁷Present address: Kafkas University, Kars, Turkey. ²⁹⁸Present address: Istanbul Bilgi University, Istanbul, Turkey. ²⁹⁹Present address: Hacettepe University, Ankara, Turkey. ³⁰⁰Present address: Istanbul University - Cerrahpasa, Faculty of Engineering, Istanbul, Turkey. ³⁰¹Present address: Vrije Universiteit Brussel, Brussel, Belgium. ³⁰²Present address: School of Physics and Astronomy, University of Southampton, Southampton, United Kingdom. ³⁰³Present address: Rutherford Appleton Laboratory, Didcot, United Kingdom. ³⁰⁴Present address: IPPP Durham University, Durham, United Kingdom. ³⁰⁵Present address: Monash University, Faculty of Science, Clayton, Australia. ³⁰⁶Present address: Università di Torino, Torino, Italy. ³⁰⁷Present address: Bethel University, St. Paul, Minneapolis, USA. ³⁰⁸Present address: Karamanoğlu Mehmetbey University, Karaman, Turkey. ³⁰⁹Present address: Bingol University, Bingol, Turkey. ³¹⁰Present address: Georgian Technical University, Tbilisi, Georgia. ³¹¹Present address: Sinop University, Sinop, Turkey. ³¹²Present address: Erciyes University, Kayseri, Turkey. ³¹³Present address: Institute of Modern Physics and Key Laboratory of Nuclear Physics and Ion-beam Application (MOE) - Fudan University, Shanghai, China. ³¹⁴Present address: Texas A&M University at Qatar, Doha, Qatar. ³¹⁵Present address: Kyungpook National University, Daegu, Korea. ³¹⁶Deceased: W. De Boer. ³¹⁷Deceased: P. Baillon. ³¹⁸Deceased: G. R. Snow.

✉ e-mail: cms-publication-committee-chair@cern.ch

Methods

Experimental set-up

The central feature of the CMS apparatus is a superconducting solenoid of 6 m internal diameter, providing a magnetic field of 3.8 T. Within the solenoid volume are a silicon pixel and strip tracker, a lead tungstate crystal electromagnetic calorimeter, and a brass and scintillator hadron calorimeter, each composed of a barrel and two endcap sections. Forward calorimeters extend the η coverage provided by the barrel and endcap detectors. Muons are measured over the range $|\eta| < 2.4$ in gas-ionization detectors, embedded in the steel flux-return yoke outside the solenoid, made using three technologies: drift tubes, cathode strip chambers and resistive plate chambers. A more detailed description of the CMS detector can be found in ref. ⁶⁴.

Events of interest are selected using a two-tiered trigger system. The first trigger level, composed of custom hardware processors, uses information from the calorimeters and muon detectors to select events at a rate of around 100 kHz with a fixed latency of about 4 μ s (ref. ⁶⁵). The second level (or high-level trigger, HLT) consists of a farm of processors running a version of the full event reconstruction software optimized for fast processing, and reduces the event rate to around 1 kHz before data storage⁶⁶. The present analysis employs an HLT that requires three muons, each having $p_T > 3.5$ GeV for $|\eta| < 1.2$ (barrel) or $p_T > 2.5$ GeV for $1.2 < |\eta| < 2.4$ (endcap). In addition, the event must have at least one pair of oppositely charged muons with invariant mass between 2.80 GeV and 3.35 GeV that originate from a common vertex with a probability greater than 0.5%, as determined by a Kalman vertex fit⁶⁷, thus suppressing random combinations of muons from unrelated sources. MC simulations are used to determine the trigger efficiency. Simulated events are generated using HELAC-Onia (v.2.6.6) with the NNPDF3.0 PDF set⁶⁸, and Pythia 8.205 for the hadronization and decay with the CUETP8M1 underlying event tune⁶². Triple- J/ψ events are simulated by combining events from two different MC samples with varying relative fractions. The first MC sample contains three singly produced J/ψ mesons, whereas the second sample combines single- and double- J/ψ meson production, following ref. ²⁸. As the J/ψ mesons originating in both processes have slightly different p_T spectra, the variation of their relative fractions in the simulation allows to effectively scan the triple-muon trigger efficiency in the more uncertain region close to the trigger p_T thresholds. The generated events are then processed through a detailed Geant4 simulation⁶⁹ of the CMS detector response.

Event reconstruction and selection

Muons are reconstructed by combining information from the silicon tracker and the muon system³⁹. The matching between tracks reconstructed in each of the subsystems proceeds either outside-in, starting from a track in the muon system, or inside-out, starting from a track provided by the silicon tracker. Matching muons to tracks measured in the silicon tracker leads to a relative p_T resolution of 1% in the barrel and 3% in the endcaps for muons with p_T up to 100 GeV (ref. ³⁹). The candidate vertex with the largest value of summed physics-object p_T^2 in the event is taken to be the PV⁷⁰. Only charged particles that are either directly participating in the PV determination, or are closest to the PV along the z direction and not used in any other PV identification (namely, they are consistent with secondary decays from the closest PV), are used in the analysis. Simulation studies show that this procedure efficiently suppresses any potential contamination from charged particles produced in any other pp collision taking place in the same bunch crossing (pile-up).

The offline data analysis starts by selecting events with six or more reconstructed muons, each passing the p_T and η criteria implemented at the HLT. The muons are combined into OS pairs, and are considered for further study if their invariant mass is $2.9 \text{ GeV} < m_{\mu^+\mu^-} < 3.3 \text{ GeV}$ (corresponding to about ± 7 times the J/ψ mass resolution discussed below) and originate from a common vertex with a probability greater than 0.5%, thereby reducing the random pairing of muons originating

from other background sources in the same event, as discussed below. All selected muon pairs are further required to share the same PV (including the possibility that they originate from secondary vertices associated to a common PV) to eliminate accidental combinations of muons from different pp collisions in the same or neighbouring bunch crossings. The analysis thereby includes prompt- J/ψ mesons coming directly from the pp interaction (or from feed-down decays of promptly produced and decayed resonances), and non-prompt ones coming from the decays of beauty hadrons. To ensure high purity and reconstruction efficiency, the J/ψ candidates are required to have $p_T > 6 \text{ GeV}$ and $|\eta| < 2.4$.

After applying the selection criteria discussed above, six triple- J/ψ events are observed. No alternative pairings among the OS muons in these six events are found to satisfy the analysis requirements. In all events, the J/ψ meson with highest p_T ('leading' J/ψ) is found to correspond to the muon pair that passed the online trigger selection. In inclusive J/ψ measurements^{23,32–35}, a continuum background is present in the $m_{\mu^+\mu^-}$ distribution due to random combinations of OS muons originating from semileptonic beauty- and charm-quark hadron decays, $b \rightarrow \mu + X$ and $c \rightarrow \mu + X$, and Drell–Yan events, which pass the trigger and data analysis criteria. To monitor the sideband background population, the mass windows corresponding to the two subleading J/ψ mesons are extended well below the J/ψ mass region. The corresponding dimuon invariant mass distributions are shown in Fig. 2 ordered (left to right) by decreasing p_T of the $\mu^+\mu^-$ system. Only one additional background event is found in the extended mass region indicated by the dotted curves, confirming that the combinatorial continuum is suppressed by the requirement of having three reconstructed J/ψ candidates in the same event.

Event kinematic properties

Detailed information of the kinematic properties of the J/ψ candidates passing the triple- J/ψ selection criteria are shown in Extended Data Table 1. The kinematic distributions of all six J/ψ triplets do not show any local peak, which could be indicative of, for example, a resonance decaying into three J/ψ mesons, but are distributed featureless (with large point-to-point statistical uncertainties) over triple- J/ψ mass, p_T and η .

All sources of systematic uncertainty in the triple- J/ψ cross-section measurement are listed in Extended Data Table 2.

Data availability

Tabulated results are provided in the HEPData record for this analysis⁷¹. Release and preservation of data used by the CMS Collaboration as the basis for publications is guided by the CMS policy as stated in [CMS data preservation, re-use and open access policy](#).

Code availability

The CMS core software is publically available at <https://github.com/cms-sw/cmssw>.

References

64. CMS Collaboration The CMS experiment at the CERN LHC. *J. Instrum.* **3**, 08004 (2008).
65. CMS Collaboration Performance of the CMS Level-1 trigger in proton–proton collisions at $\sqrt{s} = 13 \text{ TeV}$. *J. Instrum.* **15**, 10017 (2020).
66. CMS Collaboration The CMS trigger system. *J. Instrum.* **12**, 01020 (2017).
67. Frühwirth, R. Application of Kalman filtering to track and vertex fitting. *Nucl. Instrum. Methods A* **262**, 444–450 (1987).
68. Ball, R. D. et al. Parton distributions for the LHC Run II. *J. High Energy Phys.* **2015**, 040 (2015).
69. Agostinelli, S. et al. Geant4—a simulation toolkit. *Nucl. Instrum. Methods A* **506**, 250–303 (2003).

70. CMS Collaboration Particle-flow reconstruction and global event description with the CMS detector. *J. nstrum.* **12**, 10003 (2017).
71. CMS Collaboration Observation of triple J/ψ meson production in proton–proton collisions at $\sqrt{s} = 13$ TeV. *HEPData* <https://doi.org/10.17182/hepdata.114984> (2021).

Acknowledgements

We congratulate our colleagues in the CERN accelerator departments for the excellent performance of the LHC and thank the technical and administrative staffs at CERN and at other CMS institutes for their contributions to the success of the CMS effort. In addition, we gratefully acknowledge the computing centres and personnel of the Worldwide LHC Computing Grid and other centres for delivering so effectively the computing infrastructure essential to our analyses. Finally, we acknowledge the enduring support for the construction and operation of the LHC, the CMS detector, and the supporting computing infrastructure provided by the following funding agencies: BMBWF and FWF (Austria); FNRS and FWO (Belgium); CNPq, CAPES, FAPERJ, FAPERGS, and FAPESP (Brazil); MES and BNSF (Bulgaria); CERN; CAS, MoST, and NSFC (China); Minciencias (Colombia); MSES and CSF (Croatia); RIF (Cyprus); SENESCYT (Ecuador); MoER, ERC PUT and ERDF (Estonia); Academy of Finland, MEC, and HIP (Finland); CEA and CNRS/IN2P3 (France); BMBF, DFG, and HGF (Germany); GSRI (Greece); NKFI (Hungary); DAE and DST (India); IPM (Iran); SFI (Ireland); INFN (Italy); MSIP and NRF (Republic of Korea); MES (Latvia); LAS (Lithuania); MOE and UM (Malaysia); BUAP, CINVESTAV, CONACYT, LNS, SEP, and UASLP-FAI (Mexico); MOS (Montenegro); MBIE (New Zealand); PAEC (Pakistan); MSHE and NSC (Poland); FCT (Portugal);

JINR (Dubna); MON, RosAtom, RAS, RFBR, and NRC KI (Russia); MESTD (Serbia); SEIDI, CPAN, PCTI, and FEDER (Spain); MOSTR (Sri Lanka); Swiss Funding Agencies (Switzerland); MST (Taipei); ThEPCenter, IPST, STAR, and NSTDA (Thailand); TUBITAK and TAEK (Turkey); NASU (Ukraine); STFC (UK); DOE and NSF (USA). The copyright of this Article is held by CERN, for the benefit of the CMS Collaboration.

Author contributions

All authors have contributed to the publication, being variously involved in the design and the construction of the detectors, in writing software, calibrating subsystems, operating the detectors and acquiring data, and finally analysing the processed data. The CMS Collaboration members discussed and approved the scientific results. The manuscript was prepared by a subgroup of authors appointed by the collaboration and subject to an internal collaboration-wide review process. All authors reviewed and approved the final version of the manuscript.

Competing interests

The author declare no competing interests.

Additional information

Peer review information *Nature Physics* thanks Jan Kretzschmar and the other, anonymous, reviewer(s) for their contribution to the peer review of this work.

Reprints and permissions information is available at www.nature.com/reprints.

Extended Data Table 1 | Properties of J/ψ candidates measured in the triple- J/ψ events. Dimuon invariant mass, proper decay length, transverse momentum, rapidity, and azimuthal angle of each of the three J/ψ candidates measured in the six triple- J/ψ events passing our selection criteria. (The last J/ψ candidate in the last row, with invariant mass $m^{J/\psi,3}=2.94$ GeV, is likely a background event)

Event	$m^{J/\psi,1}$ (GeV)	$m^{J/\psi,2}$ (GeV)	$m^{J/\psi,3}$ (GeV)	$L^{J/\psi,1}$ (mm)	$L^{J/\psi,2}$ (mm)	$L^{J/\psi,3}$ (mm)
1	3.08	3.10	3.07	1.77	0.24	-0.01
2	3.15	3.06	3.09	0.05	0.36	0.02
3	3.10	3.14	3.11	-0.04	0.03	0.05
4	3.07	3.03	3.09	0.48	0.81	0.82
5	3.12	3.14	3.14	-0.25	0.13	-0.02
6	3.06	3.17	2.94	0.11	0.38	0.61

Event	$p_T^{J/\psi,1}$ (GeV)	$p_T^{J/\psi,2}$ (GeV)	$p_T^{J/\psi,3}$ (GeV)	$y^{J/\psi,1}$	$y^{J/\psi,2}$	$y^{J/\psi,3}$
1	17.64	17.50	8.68	-2.25	-0.39	1.53
2	91.50	54.04	11.81	1.99	0.81	-0.71
3	11.29	10.29	6.98	-0.50	-0.37	-1.64
4	15.46	10.61	7.84	-0.83	-2.24	-1.78
5	8.67	7.71	6.75	2.03	-1.14	-1.87
6	60.70	19.09	17.03	1.59	2.29	1.58

Event	$\phi^{J/\psi,1}$	$\phi^{J/\psi,2}$	$\phi^{J/\psi,3}$
1	-1.98	2.06	-1.56
2	2.60	-2.14	-0.38
3	-0.87	-1.50	0.66
4	1.00	-2.07	-1.77
5	-1.77	1.99	2.91
6	-1.98	-1.74	-2.17

Extended Data Table 2 | Systematic uncertainty contribution. Relative contributions to the systematic uncertainty of the $pp \rightarrow J/\psi J/\psi J/\psi X$ measurement. The last row gives the sum in quadrature of all components

Source	Relative uncertainty
J/ψ meson signal shape	0.8%
Dimuon continuum background shape	3.4%
Muon reconstruction and identification	1.0%
Trigger efficiency	3.4%
MC sample size	3.0%
Integrated luminosity	1.6%
Dimuon branching fraction	1.7%
Total	6.2%